

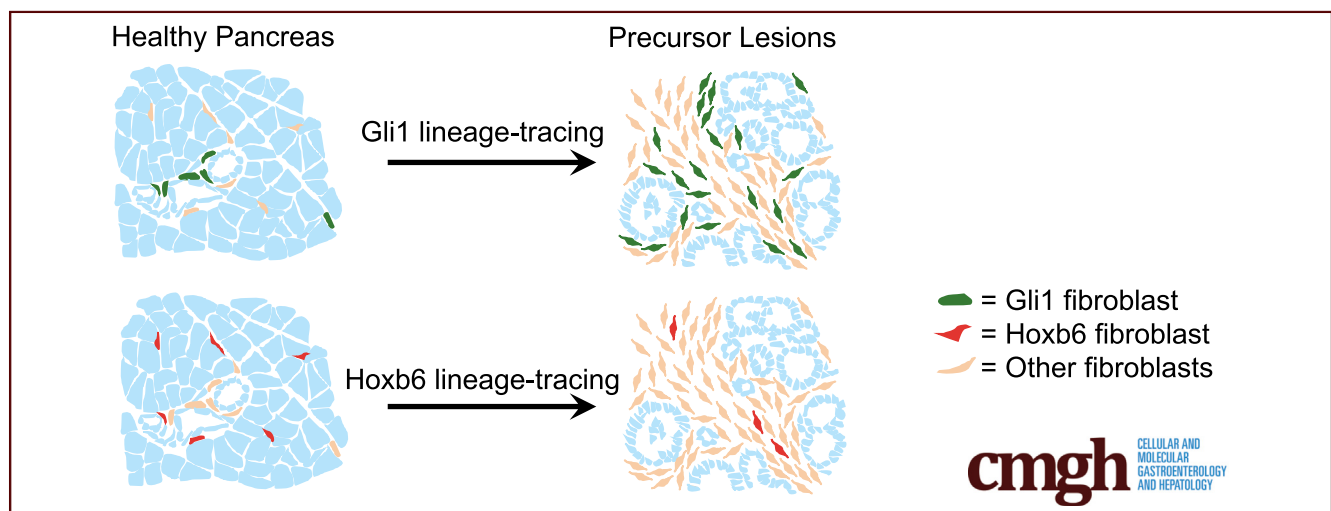
## ORIGINAL RESEARCH

## Differential Contribution of Pancreatic Fibroblast Subsets to the Pancreatic Cancer Stroma



Paloma E. Garcia,<sup>1</sup> Maeva Adoumie,<sup>2</sup> Esther C. Kim,<sup>2</sup> Yaqing Zhang,<sup>2,3</sup> Michael K. Scales,<sup>4</sup> Yara S. El-Tawil,<sup>2</sup> Amara Z. Shaikh,<sup>2</sup> Hui-Ju Wen,<sup>5</sup> Filip Bednar,<sup>2,3</sup> Ben L. Allen,<sup>3,4</sup> Deneen M. Wellik,<sup>6</sup> Howard C. Crawford,<sup>3,5,7</sup> and Marina Pasca di Magliano<sup>2,3,4</sup>

<sup>1</sup>Program in Molecular and Cellular Pathology, <sup>2</sup>Department of Surgery, <sup>3</sup>Rogel Cancer Center, <sup>4</sup>Department of Cell and Developmental Biology, <sup>5</sup>Department of Molecular and Integrative Physiology, <sup>7</sup>Department of Internal Medicine, University of Michigan, Ann Arbor, Michigan; <sup>6</sup>Department of Cellular and Regenerative Biology, University of Wisconsin–Madison, Madison, Wisconsin



## SUMMARY

The normal pancreas harbors heterogeneous fibroblast populations. Lineage tracing of these populations has shown differential contribution to the fibrotic response that accompanies pancreatic carcinogenesis. We show that Gli1 fibroblasts, which are present but rare in the normal pancreas, expand during pancreatic carcinogenesis.

**BACKGROUND & AIMS:** Although the healthy pancreas consists mostly of epithelial cells, pancreatic cancer and the precursor lesions known as pancreatic intraepithelial neoplasia, are characterized by an extensive accumulation of fibroinflammatory stroma that includes a substantial and heterogeneous fibroblast population. The cellular origin of fibroblasts within the stroma has not been determined. Here, we show that the Gli1 and Hoxb6 markers label distinct fibroblast populations in the healthy mouse pancreas. We then set out to determine whether these distinct fibroblast populations expanded during carcinogenesis.

**METHODS:** We developed genetically engineered models using a dual-recombinase approach that allowed us to induce pancreatic cancer formation through codon-optimized Flp

recombinase-driven epithelial recombination of Kirsten rat sarcoma viral oncogene homolog while labeling Gli1<sup>+</sup> or Hoxb6<sup>+</sup> fibroblasts in an inducible manner. By using these models, we lineage-traced these 2 fibroblast populations during the process of carcinogenesis.

**RESULTS:** Although in the healthy pancreas Gli1<sup>+</sup> fibroblasts and Hoxb6<sup>+</sup> fibroblasts are present in similar numbers, they contribute differently to the stroma in carcinogenesis. Namely, Gli1<sup>+</sup> fibroblasts expand dramatically, whereas Hoxb6<sup>+</sup> cells do not.

**CONCLUSIONS:** Fibroblasts present in the healthy pancreas expand during carcinogenesis, but with a different prevalence for different subtypes. Here, we compared Gli1<sup>+</sup> and Hoxb6<sup>+</sup> fibroblasts and found only Gli1<sup>+</sup> expanded to contribute to the stroma during pancreatic carcinogenesis. (*Cell Mol Gastroenterol Hepatol* 2020;10:581–599; <https://doi.org/10.1016/j.jcmgh.2020.05.004>)

**Keywords:** Cancer-Associated Fibroblasts (CAFs); Heterogeneity; Gli1; Lineage-Trace; Pancreas.

**P**ancreatic ductal adenocarcinoma (PDAC) is a deadly malignancy that is projected to become the second leading cause of cancer-related death by 2030.<sup>1</sup> The 5-year

survival rate for PDAC is only 10%, which can be attributed to the aggressive and chemoresistant nature of the cancer, in addition to the frequently late diagnosis.<sup>2</sup> In PDAC, more so than in other solid tumors, a high percentage of the tumor volume is occupied by nonmalignant cells that form the tumor stroma.<sup>3</sup> The cellular component of the stroma includes fibroblasts, infiltrating immune cells, vascular elements, and nerves.<sup>4</sup> This fibroinflammatory environment develops during the early steps of tumorigenesis and supports tumor growth and metastasis, although the roles of the individual components are still not fully understood.<sup>4</sup>

Fibroblasts are a prominent and active cellular component of the stroma; they contribute to the secretion of extracellular matrix, and produce chemokines and growth factors that affect immune, endothelial, and cancer cell growth and function.<sup>4-6</sup> Initially, research into pancreatic cancer-associated fibroblasts (CAFs) supported a unilateral protumorigenic role.<sup>7-12</sup> However, other results suggested that fibroblasts could restrain tumor formation and that depleting them might accelerate carcinogenesis.<sup>13</sup> This paradox might be explained by the observation that fibroblasts are not a homogenous population, but exist in subsets with different roles.<sup>14-17</sup>

Analysis into fibroblast heterogeneity has made considerable progress with the advent of single-cell sequencing (for review see Helms et al<sup>18</sup> and Sahai et al.<sup>19</sup> Lately, a number of research groups have identified fibroblast subpopulations, characterized by distinct patterns of gene expression, in both human and mouse PDAC tissue.<sup>20-25</sup> Even in the developing pancreas, distinct fibroblast populations were observed.<sup>26</sup> However, which type(s) of fibroblasts in the healthy pancreas gives rise to CAFs remains an open question. Although pancreatic CAFs have long been assumed to derive from the resident pancreatic stellate cells, no formal lineage tracing has been conducted to support this idea. The healthy pancreas also contains fibroblasts in peri-acinar, perivascular, and periductal regions. The potential of these resident cells in populating the fibroinflammatory environment and shaping the heterogeneity of the pancreatic cancer-associated stroma is unknown, in part because of the scarcity of markers identifying specific fibroblast populations.

Here, we describe 2 fibroblast populations that are present in the healthy pancreas, marked by the expression of Gli1 and Hoxb6. Gli1 is a zinc-finger transcription factor and downstream effector and target gene of the Hedgehog signaling pathway, which is up-regulated in human and mouse pancreatic cancer.<sup>27-29</sup> We previously described a small population of Gli1<sup>+</sup> fibroblasts in the healthy pancreas.<sup>27,30</sup> In a number of other organs, tissue-resident Gli1<sup>+</sup> cells are mesenchymal progenitors that associate closely with the vasculature until activation into proliferative myofibroblasts by injury.<sup>31-35</sup> We sought to determine whether Gli1<sup>+</sup> fibroblasts similarly proliferate in the pancreas in response to neoplasia. In contrast, Hoxb6 marks the entirety of the mesenchyme during pancreas development,<sup>36</sup> but its expression is restricted to a subset of fibroblasts in the adult pancreas. Importantly, Gli1 and Hoxb6 are expressed in largely separate populations in the healthy pancreas. We used lineage tracing and dual recombinase

approaches to follow the fate of each cell population during carcinogenesis and determined that Gli1<sup>+</sup> cells proliferated and contributed to the fibrotic reaction in pancreatic cancer, whereas Hoxb6<sup>+</sup> cells did not.


## Results

### *Gli1<sup>+</sup> Fibroblasts Are Present in the Healthy and Neoplastic Pancreas*

Pancreatic stellate cells (PSCs) have long been presumed to be the predominant mesenchymal population in the healthy pancreas.<sup>37</sup> Because Gli1<sup>+</sup> cells have not been described as stellate cells,<sup>32</sup> we sought to confirm the existence of different types of resident fibroblasts within the pancreas. PSCs, similar to hepatic stellate cells, store vitamin A in lipid droplets in the cytoplasm,<sup>38</sup> and these are visible as electron-dense inclusions in transmission electron microscopy (TEM) images. We used TEM to visualize the mesenchymal populations of the healthy mouse pancreas and observed not only PSCs (with lipid droplets) but also fibroblasts (devoid of lipid droplets) (Figure 1A).

By using a Gli1<sup>enhanced green fluorescent protein (EGFP)/+</sup> reporter, we conducted a detailed analysis of Gli1 expression in the normal pancreas, in precursor lesions called *pancreatic intraepithelial neoplasia* (PanIN), and in pancreatic cancer. First, we examined the pancreata of healthy young adult mice between 4 and 8 weeks of age that were heterozygous for Gli1<sup>EGFP/+</sup>. Gli1<sup>EGFP/+</sup> is a knock-in allele that faithfully recapitulates the expression of the endogenous locus (Figure 1B). The mice lack 1 functional allele of Gli1 but nevertheless are viable and fertile.<sup>39</sup> Because the natural fluorescence of EGFP does not persist after fixation and paraffin embedding, we used an anti-green fluorescent protein antibody to visualize the reporter expression in immunohistochemistry (IHC) or immunofluorescence (IF). We observed Gli1<sup>+</sup> cells in a perivascular location in the healthy pancreas, in a similar position previously described in the kidney, liver, lung, heart, and bone<sup>31,32,35</sup> (Figure 1C). IF staining with  $\alpha$ -smooth muscle actin ( $\alpha$ SMA) and platelet-derived growth factor receptor  $\beta$  (PDGFR $\beta$ ), both fibroblast markers, indicated that, as previously described for the Hedgehog target gene Ptch1,<sup>40</sup> Gli1 is expressed in pancreatic fibroblasts (Figure 1C). Conversely, we observed no expression of the EGFP reporter in amylase-expressing acinar cells.

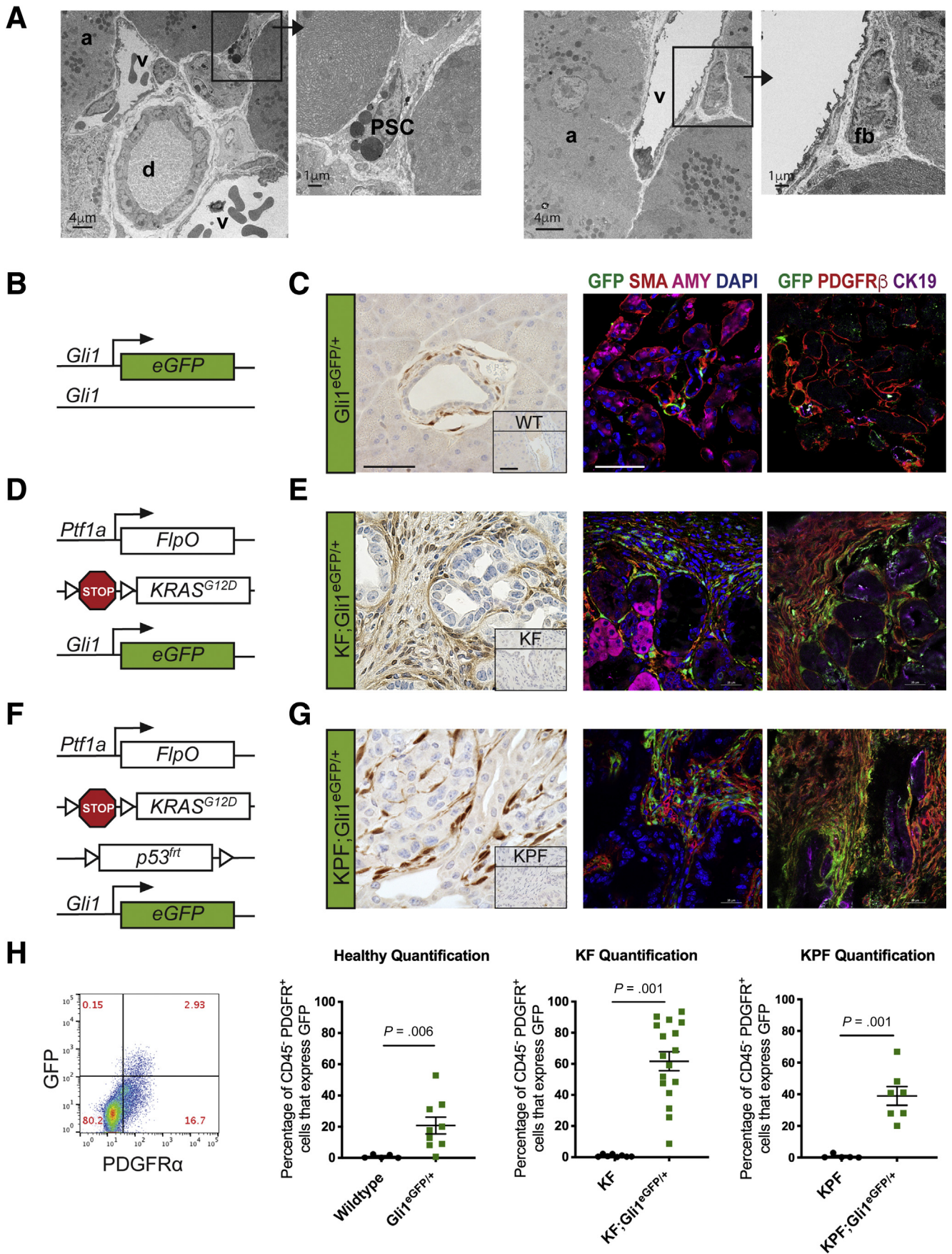
**Abbreviations used in this paper:**  $\alpha$ SMA,  $\alpha$ -smooth muscle actin; CAF, cancer-associated fibroblast; CreERT, tamoxifen-inducible Cre recombinase; EGFP, enhanced green fluorescent protein; FipO, codon-optimized Fip recombinase; IF, immunofluorescence; IHC, immunohistochemistry; KF, Ptf1a<sup>FipO/+</sup>; Kras<sup>FSF-G12D/+</sup>; KPF, Ptf1a<sup>FipO/+</sup>; Kras<sup>FSF-G12D/+</sup>; Trp53<sup>FRT-STOP-FRT/+</sup>; Kras, Kirsten rat sarcoma viral oncogene homolog; myCAF, myofibroblast cancer-associated fibroblast; PanIN, pancreatic intraepithelial neoplasia; PDAC, pancreatic ductal adenocarcinoma; PDGFR $\beta$ , platelet-derived growth factor  $\beta$ ; PSC, pancreatic stellate cell; RTom, Rosa26LSL-tdTomato; tdTomato, tandem dimer Tomato; TEM, transmission electron microscope; YFP, yellow fluorescent protein.

 Most current article

© 2020 The Authors. Published by Elsevier Inc. on behalf of the AGA Institute. This is an open access article under the CC BY-NC-ND license (<http://creativecommons.org/licenses/by-nc-nd/4.0/>).

2352-345X

<https://doi.org/10.1016/j.jcmgh.2020.05.004>



A well-established model for pancreatic carcinogenesis involves the targeted expression of mutant *Kras* in the murine pancreas. Oncogenic mutations in *Kras* are a near-universal feature of human pancreatic cancer and occur early during disease progression.<sup>41,42</sup> Expression of mutant *Kras* in genetically engineered mice leads to the formation of PanIN lesions that can progress to invasive disease over time. To evaluate Gli1 in PanIN lesions, we crossed Ptf1a-codon optimized Flp recombinase (FlpO)<sup>+/+</sup>;Kirsten rat sarcoma viral oncogene analog (*Kras*)<sup>FRT-stop-FRT (FSF)-G12D/+</sup> (KF) mice with the Gli1<sup>EGFP/+</sup> reporter, generating KF;Gli1<sup>EGFP/+</sup> mice (Figure 1D). KF mice,<sup>43</sup> similar to their counterpart Pdx1<sup>Cre</sup>;Kras<sup>loxP-stop-loxP (LSL)-G12D</sup> mice,<sup>44</sup> are born and reach adulthood with a normal pancreas, notwithstanding the expression of oncogenic *Kras*. Lesions occur spontaneously and stochastically, but can be accelerated and synchronized by the induction of acute pancreatitis.<sup>45-47</sup> Thus, we induced acute pancreatitis in KF;Gli1<sup>EGFP/+</sup> mice, and, as expected, we observed widespread PanIN development after 3 weeks. The 3-week time point was chosen because we and others have shown that this is when the pancreas parenchyma is almost completely replaced with low-grade PanIN lesions surrounded by an extensive fibroinflammatory reaction. Immunostaining for EGFP showed conspicuous positive staining limited to the stroma (Figure 1E). As in the healthy pancreas, staining was limited to the fibroblasts ( $\alpha$ SMA<sup>+</sup> and PDGFR $\beta$ <sup>+</sup> cells) and not detected in epithelial cells.

Finally, to examine Gli1 in high-grade PanINs and pancreatic cancer, we generated KF;Trp53<sup>FRT-stop-FRT/+</sup>;Gli1<sup>EGFP/+</sup> mice (Figure 1F). In these animals, FlpO recombinase activates the oncogenic *Kras* allele while also deleting 1 copy of the tumor-suppressor *Trp53*, thus essentially mimicking the commonly used KrasLSL-G12D; Trp53LSL-R172H/+; Pdx1-Cre model.<sup>48</sup> These mice lived for approximately 20 weeks, until they reached humane end points. We observed that the expression of the EGFP reporter in this cohort resembled that of low-grade lesions, with prevalent stromal expression (Figure 1G). Gli1 has been found to be expressed in epithelial cells in a variable manner across tumor lines.<sup>28,49</sup> In this advanced disease progression model, we did not observe epithelial Gli1 expression. Thus, Gli1 expression is present in a small subset of fibroblasts in the normal pancreas and becomes more prevalent in the neoplastic pancreas, and in pancreatic cancer.

We used flow cytometry and PDGFR $\alpha$  as a cell surface marker for fibroblasts to obtain a quantitative measure of Gli1<sup>+</sup> fibroblasts in the healthy and neoplastic pancreas. The

expression of EGFP was limited to PDGFR $\alpha$ <sup>+</sup> cells in healthy and neoplastic pancreata alike (Figure 1H), although we observed no or minimal expression of EGFP in CD45<sup>+</sup> immune cells (data not shown). Among PDGFR $\alpha$ <sup>+</sup> cells, the average EGFP expression was 21% in the healthy pancreas, 62% in low-grade lesions, and 39% in high-grade lesions/cancer (Figure 1H). Together, our data show that Gli1 expression is limited to a subset of fibroblasts in the healthy pancreas. In the neoplastic pancreas, Gli1 expression expands to a larger proportion of fibroblasts, a finding that might be explained by either de novo expression of Gli1 or expansion of Gli1<sup>+</sup> cells.

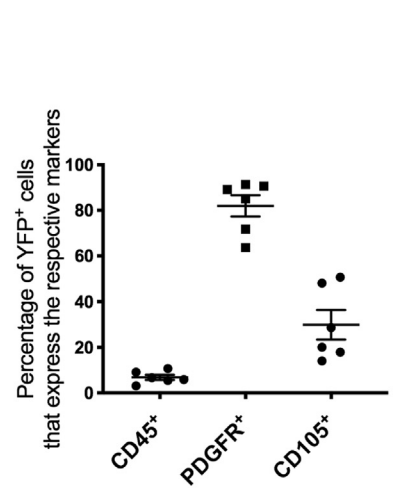
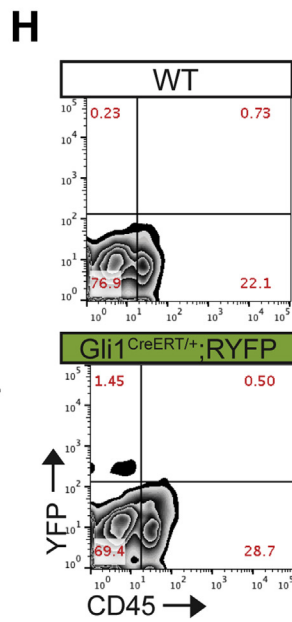
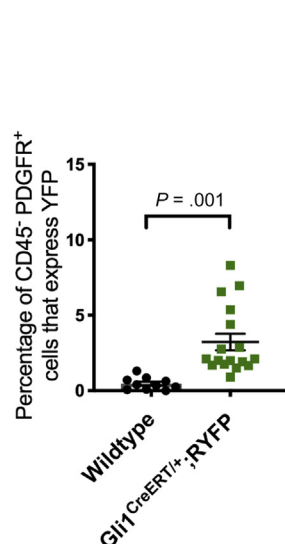
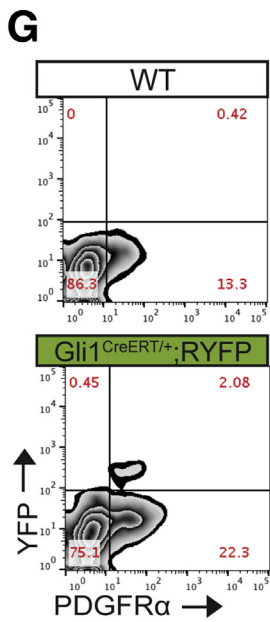
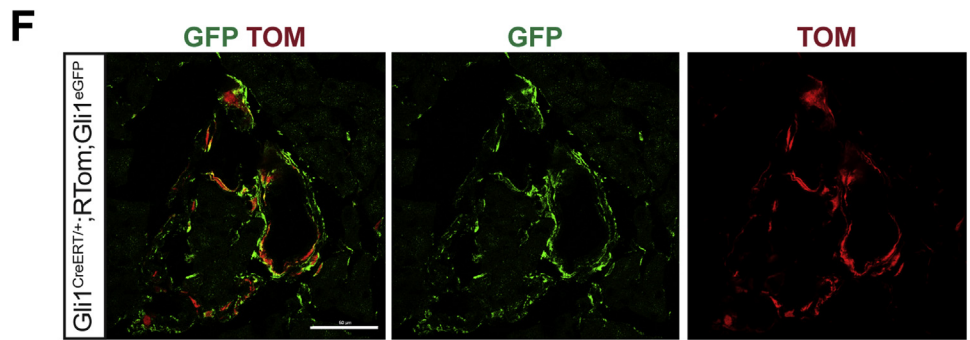
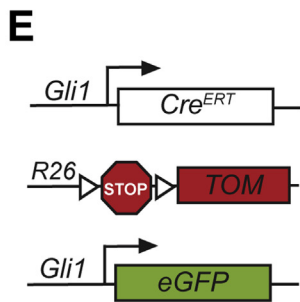
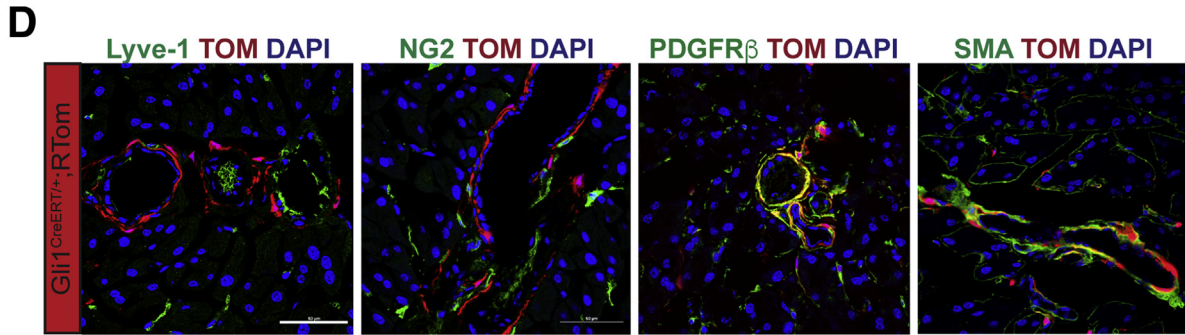
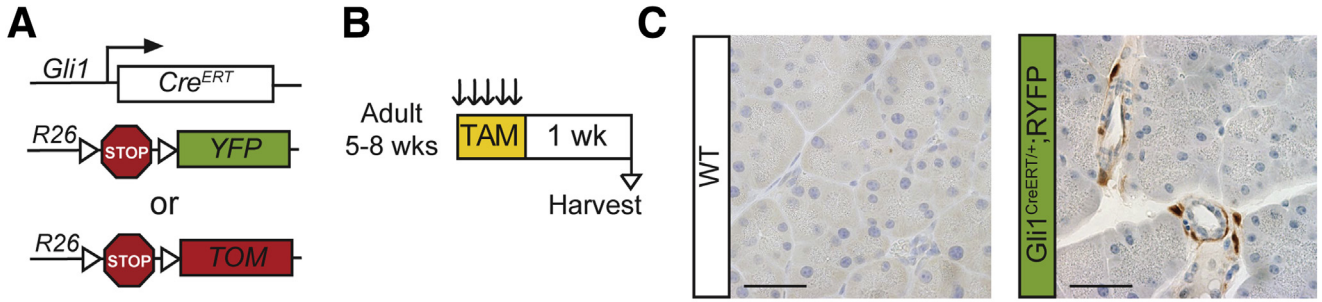
### Lineage Tracing Gli1<sup>+</sup> Fibroblasts During Carcinogenesis

We established a lineage tracing approach to follow the fate of Gli1<sup>+</sup> fibroblasts from the healthy pancreas into the diseased organ. For this purpose, we bred mice with tamoxifen-inducible Cre recombinase (CreERT) in the Gli1 locus (Gli1<sup>CreERT/+</sup>) mice with mice conditionally expressing yellow fluorescent protein (YFP) or tandem dimer Tomato (tdTomato) from the Rosa26 locus, Rosa26<sup>LSL-YFP/LSL-YFP</sup>, henceforth RYFP or Rosa26LSL-tdTomato (RTom) (Figure 2A). In the resulting dual-transgene progeny, administration of tamoxifen induced Cre recombination, permanently labeling those cells expressing Gli1 and their progeny. Importantly, labeling is transient, and thus any cell expressing Gli1 de novo, after the labeling period, would not be marked.

To examine Gli1-expressing cells in the healthy pancreas, mice aged 5–8 weeks old were administered tamoxifen daily for 5 consecutive days by oral gavage, and then analyzed a week later (Figure 2B). As expected, immunostaining for YFP in Gli1<sup>CreERT/+</sup>;RYFP mice showed an expression pattern similar to the Gli1<sup>EGFP</sup> mouse (Figure 2C). Labeled Gli1 cells often, but not exclusively, colocalized with fibroblast markers such as  $\alpha$ SMA and PDGFR $\beta$  (Figure 2D). Gli1<sup>+</sup> cells did not colocalize with Lyve-1<sup>+</sup> lymphatic endothelial cells, although they were associated closely, but not overlapping, with NG2<sup>+</sup> pericytes (Figure 2D).

We sought to evaluate the efficiency of lineage tracing in the healthy Gli1 population. We crossed Gli1<sup>CreERT/+</sup>;RTom mice into Gli1<sup>EGFP/+</sup> mice to generate Gli1<sup>CreERT/+</sup>;RTom;Gli1<sup>EGFP/+</sup> transgenic animals, which allowed us to compare the real-time expression of Gli1 with short-term lineage

**Figure 1.** (See previous page). **Gli1<sup>+</sup> fibroblasts are present in the healthy and neoplastic pancreas.** (A) TEM images of a healthy mouse pancreas. *Black squares* and *arrows* indicate sections that are magnified. (B) Genetic scheme for the knock-in Gli1<sup>EGFP/+</sup> reporter mouse. (C) Immunohistochemical staining for GFP and IF staining of GFP (green),  $\alpha$ SMA (red), and amylase (pink); and GFP (green), PDGFR $\beta$  (red), and CK19 (pink) in healthy Gli1<sup>EGFP/+</sup> mice and wild-type (*inset*) mice. *Scale bar:* 50  $\mu$ m. (D) Genetic scheme for the Ptf1a<sup>FlpO/+</sup>;Kras<sup>FRT-stop-FRT-G12D/+</sup>;Gli1<sup>EGFP/+</sup> (KF;Gli1<sup>EGFP/+</sup>) mouse. (E) IHC staining for GFP and the IF staining panels in KF;Gli1<sup>EGFP/+</sup> and KF-negative control (*inset*) mice after 3 weeks of cerulein-induced acute pancreatitis. (F) Genetic scheme for the KF;Trp53<sup>FRT-stop-FRT/+</sup>;Gli1<sup>EGFP/+</sup> (KPF;Gli1<sup>EGFP/+</sup>) mouse. (G) IHC staining for GFP and the IF staining panels in KPF;Gli1<sup>EGFP/+</sup> and KPF-negative control (*inset*) mice after evidence of disease burden. (H) Representative flow cytometry plot of GFP against PDGFR $\alpha$ , gated on 4',6-diamidino-2-phenylindole (DAPI)<sup>-</sup> CD45<sup>-</sup> cells, and quantification of the percentage of GFP<sup>+</sup> PDGFR $\alpha$ <sup>+</sup> cells at the different disease stages (n  $\geq$  5). All data are expressed as means  $\pm$  SEM. a, acinar cell; AMY, amylase; CK19, cytokeratin 19; d, duct; EGFP, enhanced green fluorescent protein; fb, fibroblast; PSC, pancreatic stellate cell; v, blood vessel.



tracing (Figure 2E). A week after tamoxifen administration, we harvested the healthy tissue and looked at the expression of the 2 fluorescent reporter genes. In this model, we found that the recombination-induced tdTomato expression was associated closely with EGFP expression (Figure 2F).

To obtain a quantitative measure of YFP in healthy  $Gli1^{CreERT/+};RYFP$  mice, we performed flow cytometry as previously described. On average, 3% of the  $PDGFR\alpha$ -positive cells were labeled by YFP (Figure 2G). Consistent with our direct reporter, immune cells ( $CD45^+$ ) did not express YFP (Figure 2H). Of the  $YFP^+$  cells, the vast majority are  $PDGFR\alpha$ -positive (82%), and approximately 30% of the  $YFP^+$  cells express CD105, a mesenchymal stromal marker (Figure 2I). Overall, our analysis showed that the  $Gli1$ - $CreERT$  allele recombined pancreatic fibroblasts, and approximately a sixth of the  $Gli1$ -expressing cells in the pancreas were labeled successfully. We estimated that this recombination efficiency was sufficient to track these cells during carcinogenesis.

### ***$Gli1^+$ Fibroblasts Expand During the Formation of Neoplastic Lesions in the Pancreas***

Now with the inducible lineage-labeling model, we sought to determine the contribution of healthy  $Gli1^+$  fibroblasts to the fibrotic reaction of PanIN development. To that end, we crossed  $Gli1^{CreERT/+};RYFP$  mice with the KF model to generate  $KF;Gli1^{CreERT/+};R26YFP$  mice (Figure 3A). We administered tamoxifen to experimental and control mice when they reached 5–8 weeks of age, which is before the occurrence of spontaneous lesions. Then, we induced acute pancreatitis and harvested the tissue 3 weeks later (Figure 3B). We found  $YFP^+$  cells to be significantly more abundant in the neoplastic tissue than in the healthy tissue when visualized and analyzed by IHC (Figure 3C and D). As in the healthy pancreas,  $Gli1$  expression was confined to the fibroblasts ( $PDGFR\beta^+$ ) and excluded from ductal or acinar epithelial cells (Figure 3E).  $Gli1^{CreERT/+};RYFP$  mice without KF alleles exposed to the same treatment fully recovered from pancreatitis, and in these tissues YFP expression resembled that of untreated healthy mice (Figure 3F).

To determine whether  $Gli1^+$  progeny persisted through cancer progression and in the context of spontaneous carcinogenesis, we generated  $Ptf1a^{FlpO/+};Kras^{FRT-stop-FRT-G12D/+}$  (KPF); $Gli1^{CreERT/+};RYFP$  mice (Figure 4A). We administered tamoxifen as these animals reached early adulthood (age, 5–8 wk), and then let them develop lesions with time (Figure 4B).

We harvested the pancreata when the mice were expected to harbor both high-grade PanIN lesions and malignant disease, approximately 18 weeks after labeling, and found abundant  $YFP^+$  cells derived from  $Gli1^+$  progenitors (Figure 4C and D).

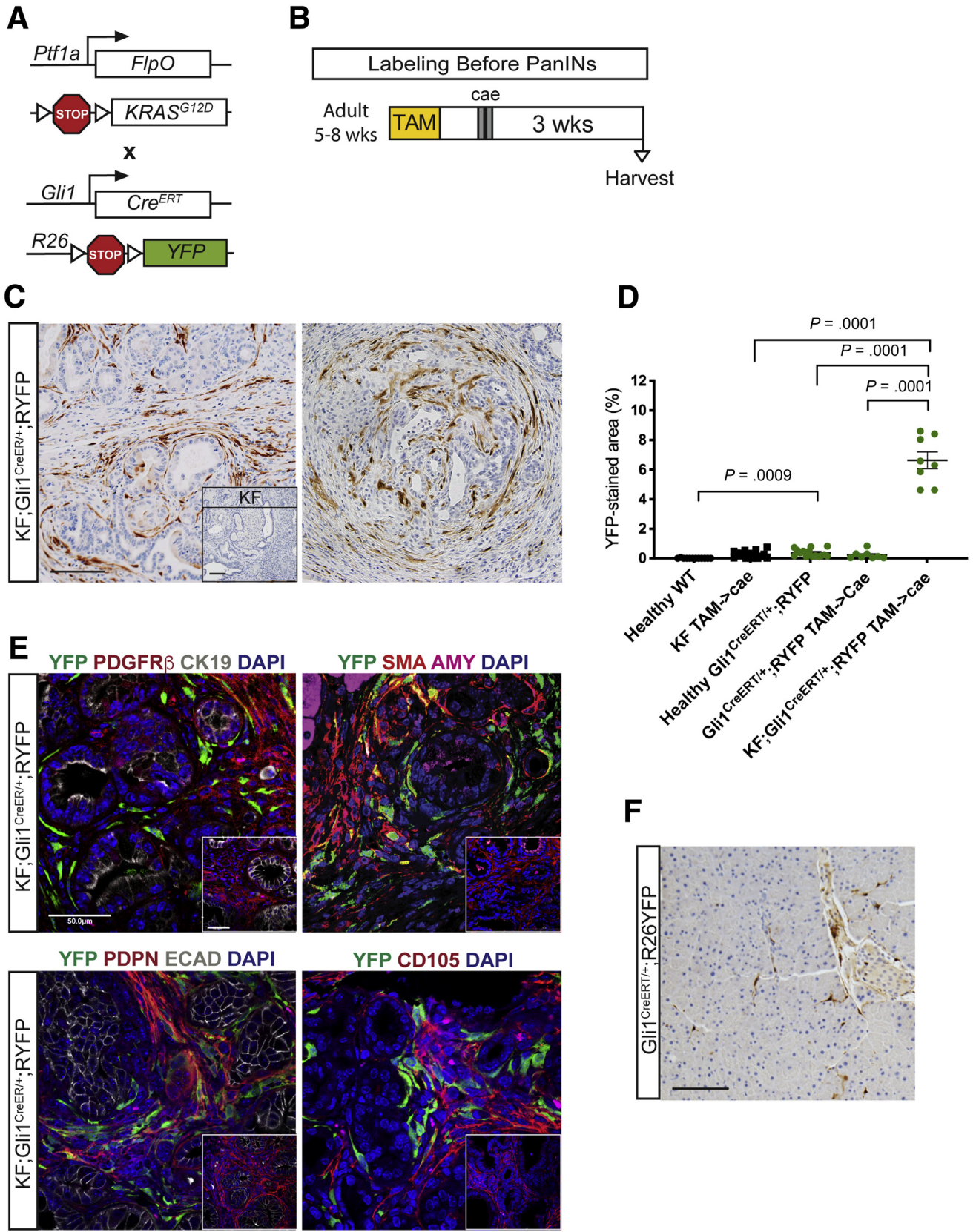
Unlike the normal pancreas, the neoplastic tissue contains a myofibroblast-like population characterized by the expression of  $\alpha SMA$ .<sup>14</sup> We observed partial co-localization of YFP and  $\alpha SMA$  in both KF and KPF lineage models (Figure 4E). By quantifying the dual IF stain, we observed lineage-traced  $Gli1^+$  cells on average contributed to a little less than half of the total myofibroblast population (Figure 4F). Conversely, the majority of our lineage-traced  $Gli1^+$  cells are myofibroblastic: an average of 70% of the  $YFP^+$  cells in both models co-expressed  $\alpha SMA$  (Figure 4F, lower panel). Thus, we showed that healthy resident  $Gli1^+$  fibroblasts expand and contribute to the  $\alpha SMA^+$  myofibroblast population during carcinogenesis.

### ***The Pancreas Is Home to Heterogeneous Fibroblast Populations That Differentially Contribute to the Neoplastic Stroma***

We then sought to determine whether all pancreatic fibroblast populations expand during carcinogenesis. For this purpose, we sought to track a different population of fibroblasts, namely  $Hoxb6^+$  cells. The homeobox factor  $Hoxb6$  is widely expressed in the mesenchyme of the developing pancreas, and regulates the embryonic development of the organ.<sup>36</sup> To assess the expression of  $Hoxb6$  in the adult pancreas, we followed a similar strategy to that described before for  $Gli1$ . We generated  $Hoxb6^{CreERT/+};RYFP$  or  $Hoxb6^{CreERT/+};RTom$  mice, administered tamoxifen once they reached adulthood, and harvested the tissues 1 week later (Figure 5A and B). Interestingly, the distribution of  $Hoxb6^+$  fibroblasts appeared different than that of  $Gli1^+$  fibroblasts, with the former being interspersed in the pancreas parenchyma, rather than concentrated around blood vessels and ducts (Figure 5C). Similar to  $Gli1$ ,  $Hoxb6$  labels a small subset of cells in the adult pancreas and is limited to fibroblasts, with no expression in other cell compartments, including endothelial cells (Figure 5D–G).

To determine whether  $Gli1^+$  and  $Hoxb6^+$  fibroblasts indeed represent different cell populations, we generated  $Hoxb6^{CreERT/+};RTom;Gli1^{EGFP/+}$  mice to dual label the populations (Figure 6A). To maximize labeling of  $Hoxb6^+$  cells, we first administered tamoxifen by oral gavage, as

**Figure 2. (See previous page). CreERT model labels healthy adult  $Gli1$ -expressing fibroblasts.** (A) Genetic scheme for  $Gli1^{CreERT/+}$  crossed with either a  $Rosa26^{YFP/+}$  or a  $Rosa26^{tdTomato/+}$  reporter. (B) Experimental design for examining healthy adult mice expressing  $Gli1$  in the pancreas. Adult mice ages 5–8 weeks were given tamoxifen gavages (4 mg/mouse/day) for 5 days. Tissue was examined 1 week after completing gavages. (C) IHC staining for YFP in healthy adult mice. Scale bar: 50  $\mu m$ . (D) IF staining of the following: Lyve-1 (green), Tomato (red), and DAPI (blue); NG2 (green), Tomato (red), and DAPI (blue);  $PDGFR\beta$  (green), Tomato (red), and DAPI (blue); and  $\alpha SMA$  (green), Tomato (red), and DAPI (blue) in  $Gli1^{CreERT/+};RTom$  samples. Scale bar: 50  $\mu m$ . (E) Genetic scheme for a  $Gli1^{CreERT/+};Gli1^{EGFP/+};RTomato$  mouse model. (F) IF staining of GFP and Tomato in the  $Gli1^{CreERT/+};Gli1^{EGFP/+};RTom$  mouse. Scale bar: 50  $\mu m$ . (G) Representative YFP vs  $PDGFR\alpha$ , flow cytometry plots of DAPI<sup>+</sup> cells in a healthy  $Gli1^{CreERT/+};RYFP$  mouse and wild-type control and the quantification ( $n \geq 10$ ). (H) Representative YFP vs  $CD45$  flow cytometry plot. (I) Quantification of the percentage of  $YFP^+$  cells that expressed  $CD45$ ,  $PDGFR\alpha$ , or  $CD105$ , as determined by flow cytometry gating. All data are expressed as means  $\pm$  SEM. TAM, tamoxifen; TOM, Tomato; WT, wild-type.



previously described, and then placed the mice on tamoxifen chow for 3 weeks before harvesting the tissue (Figure 6B). Although the low frequency of each cell population complicated the analysis, we detected single-labeled tdTomato<sup>+</sup> or EGFP<sup>+</sup> cells, and, less frequently, cells expressing both reporters (Figure 6C). To obtain a quantitative measure, we performed flow cytometry on the pancreata from mice expressing 1 or both reporters. In Hoxb6<sup>CreERT/+</sup>;RYFP mice, an average of 6% of the PDGFR $\alpha$ <sup>+</sup> fibroblasts were labeled with the reporter (Figure 5E). In the dual-labeled Hoxb6<sup>CreERT/+</sup>;RTom;Gli1<sup>EGFP/+</sup> mice, we observed closer to 20% PDGFR $\alpha$ <sup>+</sup> cells that only expressed tdTomato, the Hoxb6 marker (Figure 6D). The higher incidence of Hoxb6 in the later experiment can be attributed to the additional 3 weeks of tamoxifen chow, allowing a more complete recombination, and a stronger fluorophore to detect in flow cytometry. In the Hoxb6<sup>CreERT/+</sup>;RTom;Gli1<sup>EGFP/+</sup> mice, approximately 10% of PDGFR $\alpha$ <sup>+</sup> cells express both Hoxb6 and Gli1, although of course this number is dependent on the recombination efficacy of the inducible Cre (Figure 6D). Overall, we concluded that Hoxb6 expression sufficiently captures a healthy mesenchymal cell population within the healthy pancreas, largely distinct from fibroblasts that express Gli1.

Taking advantage of these separate fibroblast markers, we addressed whether healthy resident fibroblasts expand equally during carcinogenesis. For this purpose, we generated KF;Hoxb6<sup>CreERT/+</sup>;RYFP mice (Figure 7A). We labeled Hoxb6<sup>+</sup>-expressing cells before lesion formation, and harvested the tissue 3 weeks after inducing pancreatitis, as described earlier for Gli1<sup>+</sup>-traced animals (Figure 7B). As expected, the pancreas parenchyma in these animals was replaced by widespread PanIN lesions and surrounding stroma, and mice without KF alleles fully recovered from pancreatitis (Figure 7C). Within the stroma, labeled fibroblasts were rare (Figure 7D and E). Flow cytometry analysis confirmed these observations: although Gli1<sup>+</sup> cells give rise to an average of 14% of the fibroblasts within the stroma, Hoxb6<sup>+</sup> cells give rise to only 2% (Figure 7F).

We then altered our experimental design, inducing pancreatitis in adult mice, and then inducing Cre recombination 2 weeks later to examine the overall expression of Gli1 and Hoxb6 in PanINs, and to determine the extent of de novo expression of either marker. The pancreata were harvested 3 weeks after the induction of pancreatitis in this experiment (Figure 7G). IHC and flow cytometry analysis showed a slightly higher prevalence of Gli1<sup>+</sup> fibroblasts (an

average of 20% of PDGFR $\alpha$ <sup>+</sup> cells) than in the samples labeled before PanIN formation, suggesting that Gli1 may be activated de novo in cells that were not expressing it previously (Figure 7H and I). In contrast, the expression of Hoxb6 still was minimal and observed in only approximately 2% of the PDGFR $\alpha$ <sup>+</sup> fibroblasts.

To expand on an observation that Gli1<sup>+</sup>-traced cells often remained near neoplastic epithelial cells, we revisited the KF;Gli1<sup>CreERT/+</sup>;RYFP samples and examined areas of lesser lesion burden. In those areas, we noticed that the lineage-traced Gli1<sup>+</sup> cells often surrounded the nascent areas of acinar to ductal metaplasia and PanINs (Figure 8A). Because a subset of pancreatic fibroblasts in PDAC are described as  $\alpha$ SMA<sup>+</sup> myofibroblast-CAFs (myCAFs) and are positioned adjacent to the epithelial neoplastic cells,<sup>14</sup> we co-stained our lineage-traced Gli1<sup>+</sup> cells with  $\alpha$ SMA again. The resulting staining around these early lesions suggested occasional colocalization, but not all YFP<sup>+</sup> cells were  $\alpha$ SMA<sup>+</sup>, and not all  $\alpha$ SMA<sup>+</sup> cells were YFP<sup>+</sup> (Figure 8B). Thus, Gli1<sup>+</sup> progeny may be early contributors to the myCAF population, but even at this earliest stage, CAF heterogeneity is present.

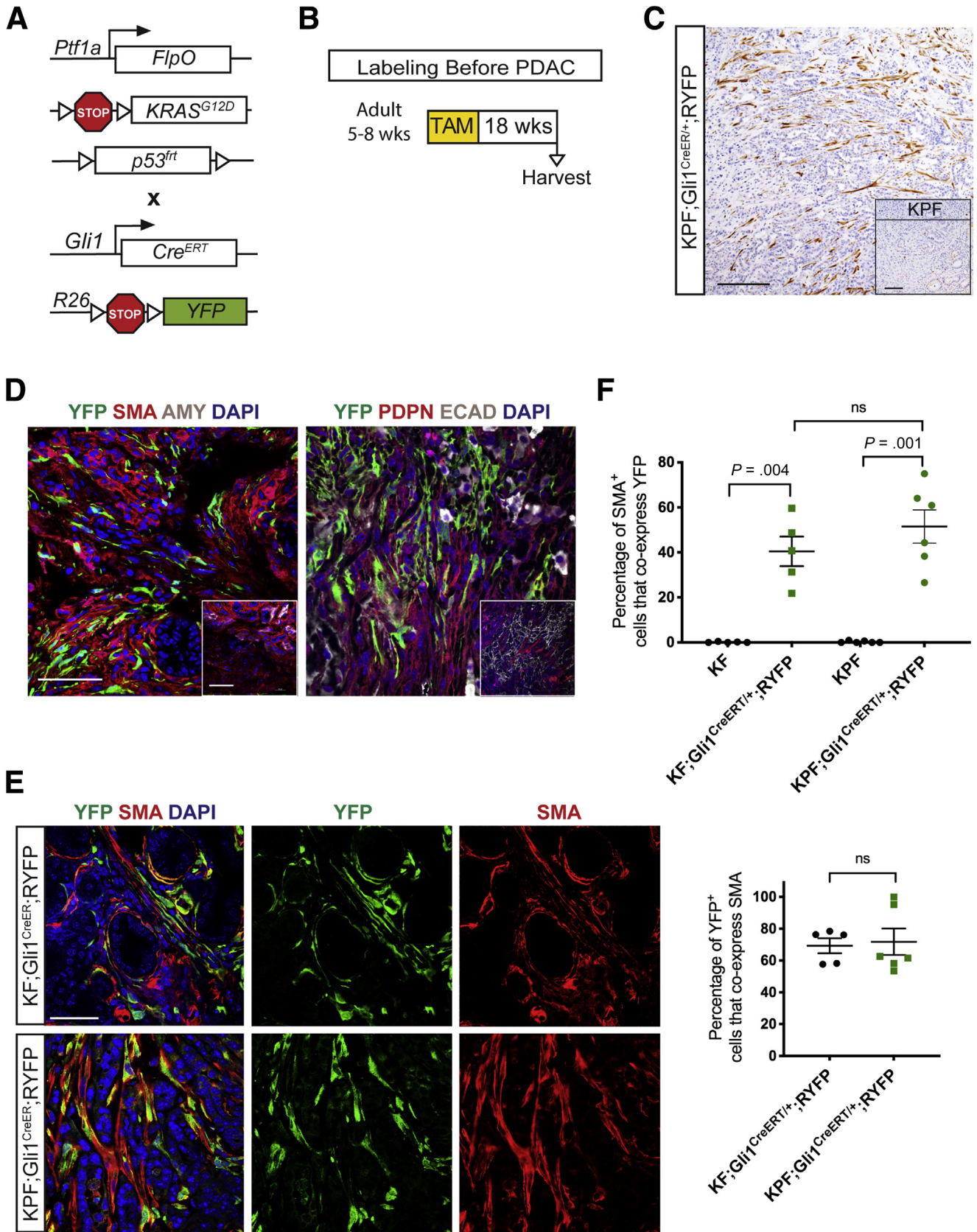
In summary, our data show that the healthy pancreas is home to heterogeneous fibroblast populations, which have a differential potential to expand during the process of carcinogenesis. Although we were able to lineage trace 2 of these populations, our data also indicate that other progenitors for the fibrotic stroma must exist to contribute to the remaining fibroblast populations.

## Discussion

In the pancreas, the mesenchyme surrounds and supports epithelium development<sup>50</sup> and differentiates to form cell types such as fibroblasts, pancreatic stellate cells, and pericytes.<sup>51,52</sup> Activated fibroblasts, also known as myofibroblasts, help regulate wound repair and recovery,<sup>53,54</sup> but in the context of certain pancreatic diseases, such as chronic pancreatitis and pancreatic cancer, the fibrosis is not resolved. Fibroblasts thus are an abundant, active, and heterogeneous player within the tumor microenvironment of pancreatic adenocarcinoma. Currently, functionally distinct subclasses of CAFs have been defined in other cancers such as breast carcinoma,<sup>55,56</sup> colorectal carcinoma,<sup>57</sup> and lung adenocarcinoma.<sup>58</sup> In pancreatic cancer, a putative mesenchymal stem cell population has been identified in mouse and human samples,<sup>16,17</sup> and CAFs have been classified into myCAF, inflammatory-CAF, and antigen-presenting-CAF (apCAF)

**Figure 3. (See previous page). Gli1<sup>+</sup> fibroblasts lineage-traced before pancreatitis-induced PanIN lesion formation contribute to the stroma.** (A) Genetic scheme for a KF;Gli1<sup>CreERT/+</sup>;RYFP mouse. (B) Experimental design for labeling healthy Gli1<sup>+</sup> cells before PanIN generation. Adult mice 5–8 weeks old were given 5 tamoxifen gavages and rested for a week before 2 days of cerulein injections to induce pancreatitis. After 3 weeks, samples were collected. (C) IHC staining for YFP in KF;Gli1<sup>CreERT/+</sup>;RYFP and KF control tissue (*inset*) labeled before PanIN generation. Scale bar: 100  $\mu$ m. (D) Quantification of YFP<sup>+</sup> staining area from IHC ( $n \geq 8$ ) (E) IF staining on KF;Gli1<sup>CreERT/+</sup>;RYFP and KF control (*inset*) samples of YFP (green), PDGFR $\beta$  (red), cytokeratin 19 (CK19) (white), and 4',6-diamidino-2-phenylindole (DAPI) (blue); YFP (green),  $\alpha$ SMA (red), amylase (pink), and DAPI (blue); YFP (green), podoplanin (red), E-cadherin (white), and DAPI (blue); and YFP (green), CD105 (red), and DAPI (blue). Scale bar: 50  $\mu$ m. (F) A representative YFP IHC image of a Gli1<sup>CreERT/+</sup>;RYFP mouse that followed the same labeling scheme. Scale bar: 100  $\mu$ m. AMY, amylase; ECAD, E-cadherin; TAM, tamoxifen; WT, wild-type.





populations with potentially distinct functions and activation pathways.<sup>14,15,20</sup>

Here, we sought to determine which fibroblasts in the healthy pancreas give rise to CAFs during the progression of carcinogenesis. A population of pancreatic stellate cells, containing lipid droplets with vitamin A deposits, similar to liver hepatic stellate cells, has been described,<sup>37,59,60</sup> and traditionally is considered the source of the fibrotic reaction in pancreatic cancer. However, no experimental validation supports the notion that stellate cells lead to CAFs. Recent single-cell transcriptomic profiles of healthy or low-grade lesion fibroblast populations have been mapped *in silico* to CAFs, which suggests that resident pancreatic fibroblasts do contribute to CAFs.<sup>23,25</sup> To directly trace resident fibroblast populations, however, we first needed to define markers of distinct populations of fibroblasts.

We characterized 2 different populations of pancreatic fibroblasts present in the healthy organ by the expression of the transcription factors Gli1 and Hoxb6. Gli1 is a target gene and transcriptional effector of the Hedgehog signaling pathway (see Lau et al<sup>29</sup> and Hui et al<sup>61</sup>). Hedgehog signaling is active throughout embryonic development of the gastrointestinal tract, but needs to be suppressed to allow for the formation of the pancreas anlage.<sup>61–63</sup> However, some low level of Hedgehog signaling persists<sup>64</sup> to maintain homeostasis and assist in injury recovery.<sup>32,65,66</sup> Thus, we found that a subset of fibroblasts in the healthy pancreas consistently express Gli1 and do not have characteristics of stellate cells. Meanwhile, Hoxb6 is expressed throughout the mesenchyme of the developing pancreas,<sup>36</sup> and in a portion of fibroblasts in the adult organ. Although there is partial overlap in Gli1- and Hoxb6-expressing cells, largely they consist of separate populations. We thus set out to lineage trace these populations with the goal to answer the following questions: (1) whether either fibroblast population gives rise to CAFs; (2) whether all fibroblast populations expand during carcinogenesis; and (3) whether different functional CAF subpopulations derive from different progenitors in the healthy pancreas.

Gli1<sup>+</sup> fibroblasts have been lineage-traced in several organ fibrosis models. After injury, the majority of Gli1<sup>+</sup> cells acquire  $\alpha$ SMA expression and contribute to fibrosis. Approximately 40% of myofibroblasts in the kidney, liver, and lung, and 60% of myofibroblasts in the heart originated from tissue-resident Gli1<sup>+</sup> progenitors after a fibrosis-inducing injury.<sup>32,33</sup> In addition, Gli1 progenitors contribute approximately half of the myofibroblasts in

instances of endochondral heterotopic ossification and bone marrow fibrosis.<sup>31,35</sup> Gli1<sup>+</sup> fibroblasts have not been characterized in the pancreas, and their contribution to tumor-associated fibroblasts has not yet been studied. We found Gli1 to be expressed in a minority of healthy PDGFR $\alpha$ <sup>+</sup> fibroblasts and localized in a perivascular position adjacent to pericytes. When we lineage-traced the progeny of healthy Gli1<sup>+</sup> fibroblasts, we found they expanded in quantity and contributed to CAFs.

Hoxb6 is a developmental transcription factor expressed prominently in the pancreas mesoderm until embryonic day 16.5.<sup>36</sup> We showed that Hoxb6 expression is present in the healthy mouse pancreas in a portion of PDGFR $\alpha$ <sup>+</sup> fibroblasts, but not in immune cells. We had hypothesized that this fibroblast subpopulation would expand and contribute to the fibrotic stroma in a similar manner as the Gli1<sup>+</sup> population owing to the relative prevalence of the cells and the occasional overlap between Hoxb6 and Gli1 expression. Interestingly, as we lineage-traced Gli1 and Hoxb6 cells from the healthy pancreas into carcinogenesis, we found that they contributed in a very different manner to the stroma. Although Gli1<sup>+</sup> fibroblasts expanded during carcinogenesis, Hoxb6<sup>+</sup> cells failed to do so. Furthermore, the expression of Gli1 was extensive in lesions and advanced disease, while Hoxb6 expression did not increase.

Our findings suggest that not all resident fibroblast populations expand and transition into cancer-associated fibroblasts within the pancreas, and that fibroblasts are heterogeneous with separate functional roles even at the healthy stage. Gli1<sup>+</sup> cells likely are contributing to a portion of the tumor-associated myCAF population, although it is worth noting that even within the Gli1<sup>+</sup> cells of the healthy pancreas, there is heterogeneity. For instance, a subset of Gli1 and Hoxb6 cells express CD105, a mesenchymal stromal marker. This could indicate heterogeneity or perhaps a distinct activation state within the population. In addition, a subset of Gli1<sup>+</sup> cells express Hoxb6. This dual-positive population does not appear to proliferate because we observed minimal Hoxb6<sup>+</sup> fibroblasts among the PanIN stroma when we lineage-traced Hoxb6<sup>+</sup> cells. However, Hoxb6<sup>+</sup> fibroblasts conceivably could be proliferating and dying before our analysis time points. Unfortunately, because Hoxb6 has close homology with other homeobox genes, further antibody or RNA-based investigation is hindered. Instead, further investigation into the fate, function, and drivers of other fibroblast populations is needed to best comprehend the complexity of the fibrotic reaction. Different CAF subpopulations may

**Figure 4.** (See previous page). Gli1<sup>+</sup> fibroblasts contribute to the stroma when lineage-traced in a spontaneous pancreatic carcinogenesis model. (A) Genetic scheme for a KPF;Gli1<sup>CreERT/+</sup>;RYFP mouse. (B) Experimental design for labeling healthy Gli1<sup>+</sup> cells before spontaneous carcinogenesis. Adult mice 5–8 weeks old were given 5 tamoxifen gavages, aged, and then harvested on evidence of disease burden. (C) IHC staining for YFP in KPF;Gli1<sup>CreERT/+</sup>;RYFP and KPF control (*inset*) mice. Scale bar: 100  $\mu$ m. (D) IF staining for YFP (green),  $\alpha$ SMA (red), amylase (gray), and DAPI (blue); and YFP (green), podoplanin (red), E-cadherin (white), and DAPI (blue) in KPF;Gli1<sup>CreERT/+</sup>;RYFP and KPF control (*inset*) samples. Scale bar: 50  $\mu$ m. (E) Merged and single-channel IF images for YFP (green),  $\alpha$ SMA (red), and DAPI (blue) in KF and KPF Gli1<sup>CreERT/+</sup>;RYFP samples. Scale bar: 50  $\mu$ m. (F) IF quantification of the percentage of  $\alpha$ SMA<sup>+</sup> cells that co-expressed YFP in lineage-traced KF and KPF samples (n  $\geq$  5). (G) IF quantification of the percentage of YFP<sup>+</sup> cells that co-expressed  $\alpha$ SMA in lineage-traced KF and KPF samples (n  $\geq$  8). All data are expressed as means  $\pm$  SEM. AMY, amylase; TAM, tamoxifen.

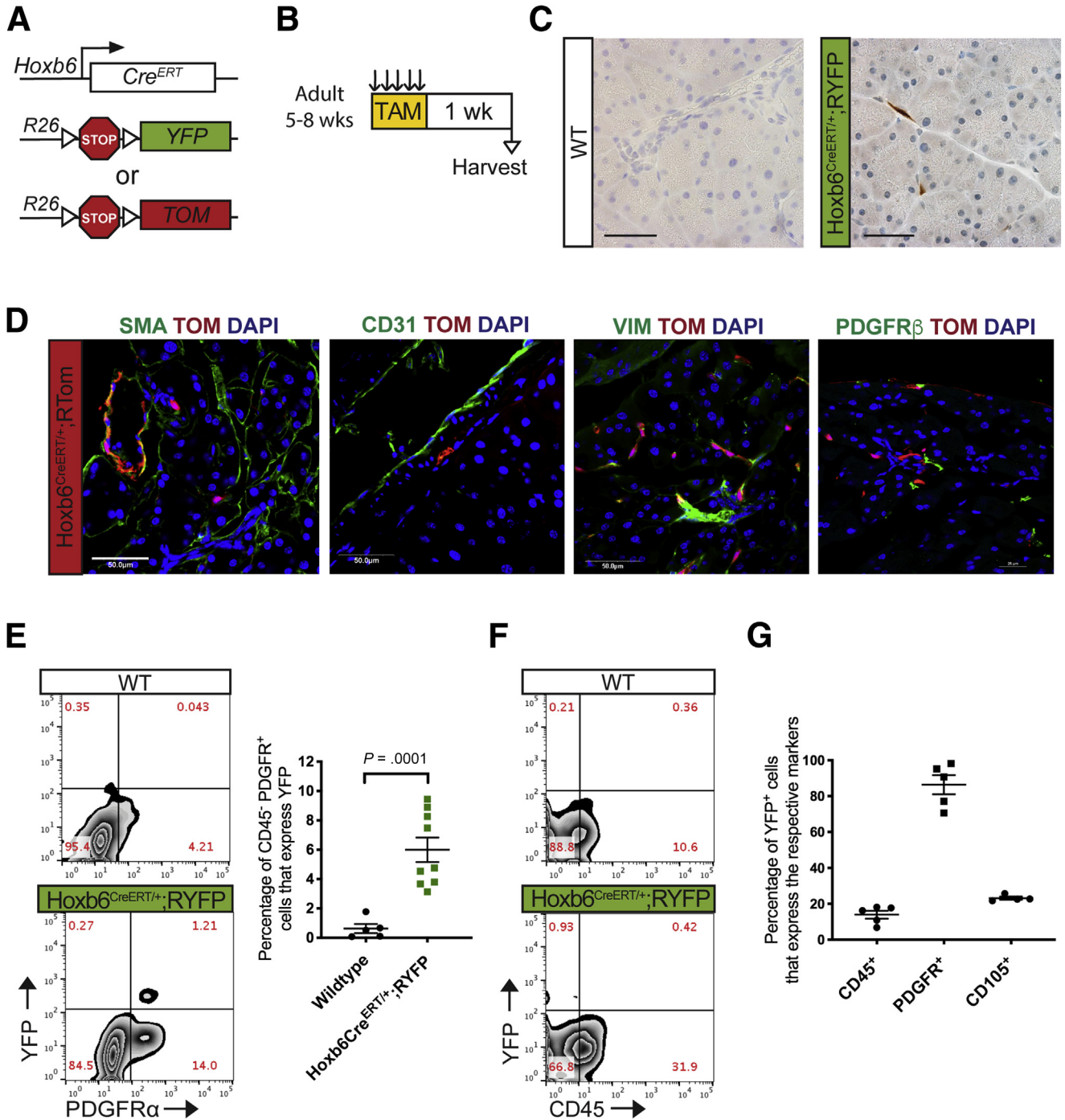


**Figure 5. Hoxb6 labels a subset of mesenchymal cells in the healthy pancreas.** (A) Genetic scheme for Hoxb6<sup>CreERT/+</sup> crossed with either a RYFP reporter or RTomato reporter. (B) Experimental protocol for examining healthy adult mice expressing Hoxb6 in the pancreas. Adult mice aged 5–8 weeks were given tamoxifen gavages (4 mg/mouse/day) for 5 days. Tissue was examined 1 week after completing gavages. (C) IHC staining for YFP in healthy adult mice. Scale bar: 50  $\mu$ m. (D) IF staining of  $\alpha$ SMA (green), Tomato (red), and 4',6-diamidino-2-phenylindole (DAPI) (blue); CD31 (green), Tomato (red), and DAPI (blue); vimentin (green), Tomato (red), and DAPI (blue); and PDGFR $\beta$  (green), Tomato (red), and DAPI (blue) in healthy Hoxb6<sup>CreERT/+</sup>;RTom tissue. Scale bar: 50  $\mu$ m. (E) Representative YFP vs PDGFR $\alpha$ <sup>+</sup> flow cytometry plots of DAPI<sup>-</sup> cells in a Hoxb6<sup>CreERT/+</sup>;RYFP mouse and wild-type control and the quantification (n  $\geq$  5). (F) Representative YFP vs CD45 flow cytometry plot. (G) Quantification of the percentage of YFP<sup>+</sup> cells that expressed CD45, PDGFR $\alpha$ , or CD105 as determined by flow cytometry gating. All data are expressed as means  $\pm$  SEM. TAM, tamoxifen; VIM, vimentin; WT, wild-type.

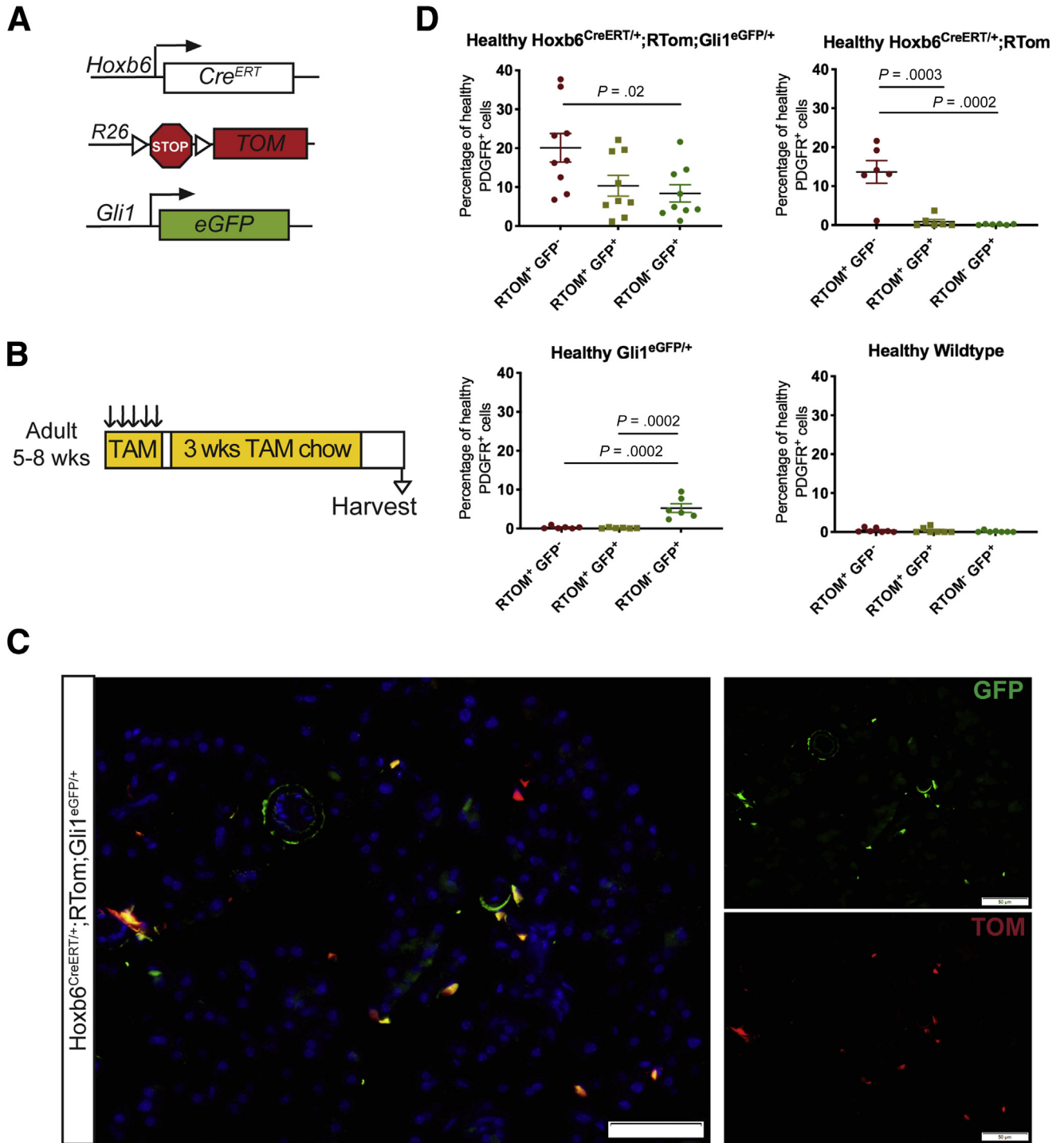
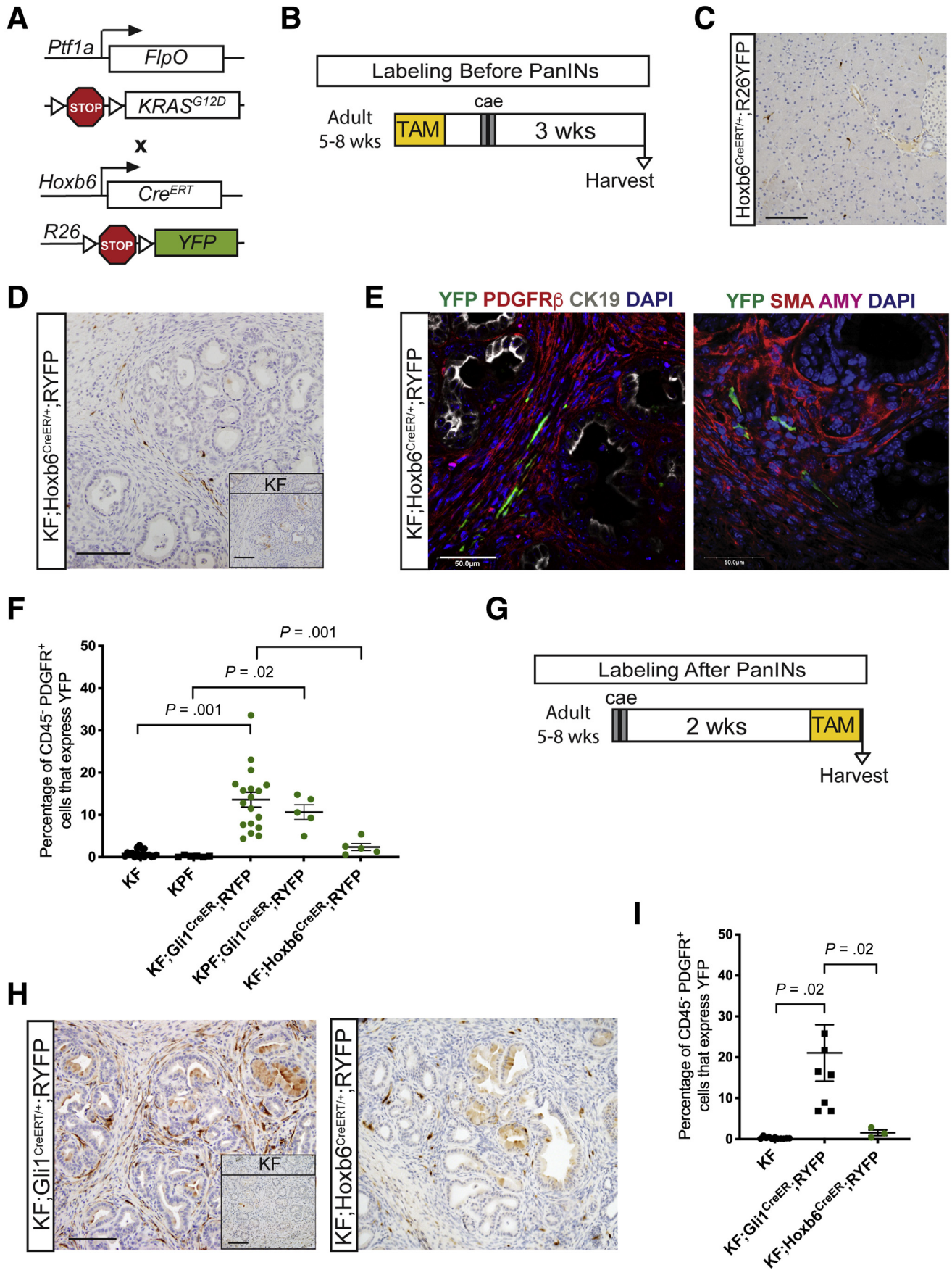


**Figure 6. Hoxb6 and Gli1 are expressed in different populations.** (A) Genetic scheme for a  $Hoxb6^{CreERT/+};RTom;Gli1^{eGFP/+}$  mouse model. (B) Experimental design for examining healthy  $Hoxb6^{CreERT/+};RTom;Gli1^{eGFP/+}$  mice. Adult mice aged 5–8 weeks were given tamoxifen gavages (4 mg/mouse/day) for 5 days. Mice then were placed on tamoxifen chow for 3 weeks. Tissue was examined 1 week after completing chow regimen. (C) IF staining of GFP and Tomato in the  $Hoxb6^{CreERT/+};RTom;-Gli1^{eGFP/+}$  mouse. Scale bar: 50  $\mu m$ . (D) Flow cytometry quantification of the percentage of healthy  $CD45^{-}PDGFR\alpha^{+}$  cells that expressed Tomato, GFP, or both ( $n \geq 6$ ). All data are expressed as means  $\pm$  SEM. RTOM, Rosa26LSL-tdTomato; TAM, tamoxifen.



derive from different progenitors, as suggested in an experiment in which the single-cell transcriptional profiles of 2 healthy fibroblast populations mapped closer to the tumor-associated myCAF or inflammatory-CAF populations than to themselves.<sup>23</sup>

Understanding the complexity of fibroblasts in healthy organs and disease has been hampered by the limited availability of specific markers. Pancreatic cancer fibroblasts have long been assumed to derive from resident stellate cells,<sup>37</sup> with no *in vivo* experimental support. Here, we show that nonstellate cell fibroblast populations exist in the pancreas and they have the ability to expand during carcinogenesis. In addition, we determined that the ability to contribute to the cancer-associated stroma during carcinogenesis is unique to only some fibroblast subsets in the pancreas. We found Gli1<sup>+</sup> fibroblasts gave rise to less than half of the total fibroblast population during carcinogenesis. This is likely a conservative figure based on imperfect recombination efficiency, but it nonetheless indicates that other subsets must exist in the healthy organ with the ability to expand. Alternative sources of the CAFs may arise from other resident fibroblast populations, circulating progenitor cells from the bone marrow, or pericytes (reviewed by LeBleu<sup>6</sup> and El Agha<sup>67</sup>). Overall, these findings are consistent with fate-mapping experiments performed in the liver,<sup>32,68</sup> kidney,<sup>32,69</sup> heart,<sup>32,70</sup> lung,<sup>32,71,72</sup> spinal cord,<sup>73</sup> bone,<sup>31</sup> and skin,<sup>74</sup> in which resident fibroblasts proliferate in response to injury to contribute, at least partially, to organ fibrosis. Our findings advance our understanding of how the pancreatic fibroinflammatory environment is established during carcinogenesis and offer new directions with which to examine the main stromal regulators of carcinogenesis, and, eventually, improve patient outcome.

## Materials and Methods

### Mouse Strains

All mouse protocols were conducted with approval from the University Committee on Use and Care of Animals. Gli1<sup>EGFP/+</sup> mice<sup>75</sup> were crossed with KF or KPF mouse models donated by Dr Crawford<sup>43</sup> to generate KF;Gli1<sup>EGFP/+</sup> and KPF;Gli1<sup>EGFP/+</sup> crosses. Gli1<sup>CreERT/+</sup> (The Jackson Laboratory, Bar Harbor, ME, #007913) or Hoxb6<sup>CreERT/+</sup> (contributed by Dr Wellik<sup>76</sup>) mice were crossed into Rosa26<sup>YFP/+</sup> (The Jackson Laboratory, #006148) or

Rosa26<sup>Tom/+</sup> (The Jackson Laboratory, #007909) reporter mice. These mice then were crossed further with the KF and KPF mice. Experimental and control animals were treated in parallel. Mice were housed in specific pathogen-free facilities at the University of Michigan Rogel Cancer Center.

### In Vivo Experiments

All experiments were initiated in adult mice between 5 and 8 weeks of age. Acute pancreatitis was induced over 2 days. For 8 hours each day, mice received hourly intraperitoneal injections of cerulein (Sigma-Aldrich, St. Louis, MO) as previously described.<sup>47,77</sup> To activate the CreERT transgene, mice received 4 mg tamoxifen in corn oil/3% ethanol (Sigma-Aldrich) per day via oral gavage for 5 days. Where mentioned, mice received an additional 3 weeks of tamoxifen chow (400 tamoxifen citrate mg/kg diet; Envigo, Indianapolis, IN).

### Immunohistochemistry and Immunofluorescence

All immunohistochemical and immunofluorescent stains were performed as previously described.<sup>78</sup> Primary antibodies used were as follows: YFP (1:200; Abcam, Cambridge, MA), PDGFR $\beta$  (1:100; Abcam), cytokeratin 19 (1:50; Iowa Developmental Hybridoma Bank, Iowa City, IA),  $\alpha$ SMA (1:1000; Sigma-Aldrich), amylase (1:100; Sigma), epithelial cell adhesion molecule (1:300; Cell Signaling, Danvers, MA), podoplanin (1:300; BioLegend, San Diego, CA), CD31 (1:50; Cell Signaling), vimentin (1:100; Cell Signaling), neuron-glial antigen (1:100; Abcam), and lymphatic vessel endothelial receptor 1 (1:100; Abcam). Images were taken with an Olympus BX-51 microscope, and CellSens (Olympus, Center Valley, PA) standard software. For IF, Alexa Fluor-conjugated (Invitrogen, Carlsbad, CA) secondary antibodies were used. Prolong Gold-4',6-diamidino-2-phenylindole (Invitrogen) was used to counterstain the cell nuclei. The images were acquired using a Nikon A1 inverted confocal microscope and NIS-Elements software (Nikon, Melville, NY). At least 5 separate 60 $\times$  fields (>180 cells) for IF or 20 $\times$  fields for IHC from more than 1 experimental sample were quantified using HALO software (Perkin Elmer, Waltham, MA).

### TEM

Tissues for transmission electron microscope analysis were prepared by the University of Michigan Microscopy

**Figure 7. (See previous page). Hoxb6<sup>+</sup> fibroblasts do not contribute to the pancreatic stroma.** (A) Genetic scheme for the KF;Hoxb6<sup>CreERT/+</sup>;RYFP model. (B) Experimental design for labeling healthy Hoxb6<sup>+</sup> cells before PanIN generation. Adult mice 5–8 weeks old were given 5 tamoxifen gavages and rested a week before 2 days of cerulein injections to induce pancreatitis. After 3 weeks, mice were harvested. (C) A representative YFP IHC image of a Hoxb6<sup>CreERT/+</sup>;RYFP mouse following the protocol. Scale bar: 100  $\mu$ m. (D) IHC staining for YFP in KF;Hoxb6<sup>CreERT/+</sup>;RYFP and KF control (*inset*) mice labeled before PanIN generation. Scale bar: 100  $\mu$ m. (E) IF staining panels of YFP (green), PDGFR $\beta$  (red), cytokeratin 19 (CK19) (white), DAPI (blue); and YFP (green),  $\alpha$ SMA (red), amylase (pink), and DAPI (blue) in KF;Hoxb6<sup>CreERT/+</sup>;RYFP mice labeled before PanIN generation. Scale bar: 50  $\mu$ m. (F) Flow cytometry quantification of the percentage of CD45<sup>-</sup>PDGFR<sup>+</sup> cells that expressed YFP in lineage-traced Gli1 and Hoxb6 mice and their controls (n  $\geq$  5). (G) Experimental design for labeling after PanIN generation. Adult mice 5–8 weeks old were given cerulein injections, rested for 2 weeks, and then given 5 gavages of tamoxifen before tissue collection. (H) IHC staining for YFP in KF;Gli1<sup>CreERT/+</sup>;RYFP and KF;Hoxb6<sup>CreERT/+</sup>;RYFP mice labeled after PanIN generation. *Inset* shows KF control. Scale bar: 100  $\mu$ m. (I) Flow cytometry quantification of the percentage of CD45<sup>-</sup>PDGFR<sup>+</sup> cells that express YFP in KF;Gli1<sup>CreERT/+</sup>;RYFP and KF;Hoxb6<sup>CreERT/+</sup>;RYFP mice labeled after PanIN generation (n  $\geq$  3). All data are expressed as means  $\pm$  SEM. AMY, amylase.

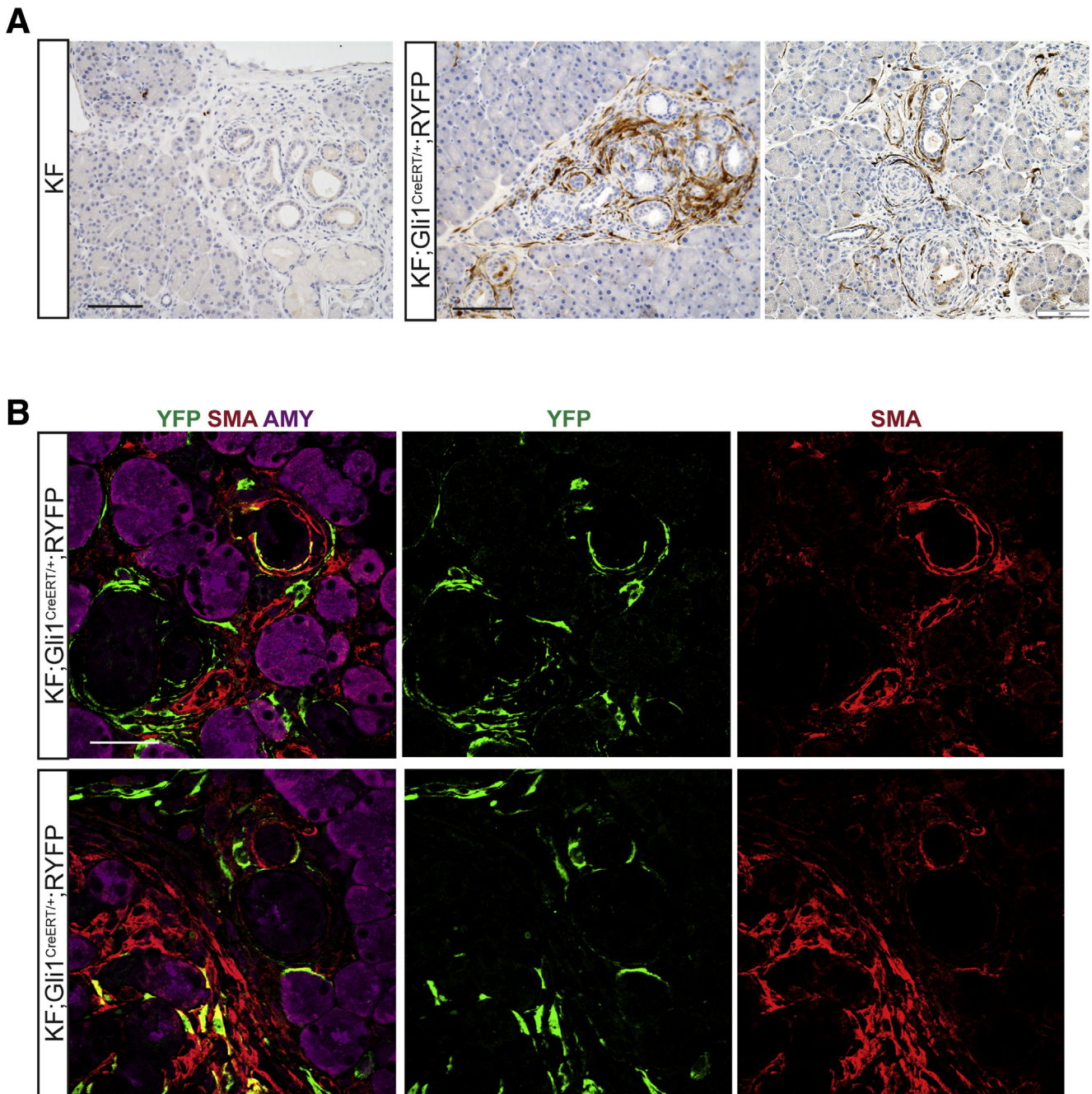


**Figure 8. Lineage-traced *Gli1* fibroblasts are present around the earliest lesion development.** (A) IHC staining for YFP in KF;Gli1<sup>CreERT+/+</sup>;RYFP mice labeled before PanIN generation. Scale bar: 100  $\mu$ m. (B) IF merged and single-channel images for YFP (green),  $\alpha$ SMA (red), and amylase (pink) in KF;Gli1<sup>CreERT+/+</sup>;RYFP mice. Scale bar: 50  $\mu$ m. AMY, amylase.

Core and images were acquired using a Philips CM-100 transmission electron microscope (FEI, Hillsboro, Oregon).

### Flow Cytometry

Pancreatic single-cell suspensions were prepared as described<sup>79</sup> by mincing the tissue and then digesting in 1 mg/mL collagenase V (Sigma-Aldrich) at 37°C for 15–20 minutes. Digested samples were filtered through a 40- $\mu$ m strainer and subjected to a red blood cell lysis step.

Samples were submitted for flow analysis in Hank's balanced salt solution with 2% fetal bovine serum. Antibodies were used in combinations of the following: CD45-Pacific Orange (1:50; BD Pharmingen, Franklin Lakes, NJ), PDGFR $\alpha$ -Phycoerythrin (1:50; BD Pharmingen), and PDGFR $\alpha$ -Phycoerythrin-Cy7 (1:50; BD Pharmingen). Fluorescence-activated cell sorting was performed on a MoFlo Astrios (Beckman Coulter) and data were analyzed using Summit 6.1 Software (Beckman Coulter, Brea, CA) and Flowjo 10.6 (Flowjo, Ashland, OR).

The gating strategy was as follows: cells were first selected on forward (FSC-Area) and side (SSC-Area) scatters to exclude debris. Then single cells were gated based on SSC-Height vs SSC-Width and FSC-Height vs FSC-Width parameters. Alive cells were selected from an SSC-Height vs 4',6-diamidino-2-phenylindole plot. Nonimmune cells were selected from an SSC-Height vs CD45-Pacific Orange plot. At least  $1 \times 10^5$  events that pass these selection parameters were recorded for each sample. Further gating based on PDGFR, YFP, and Tomato parameters was used to analyze and sort the cells.

### Statistical Analysis

The Student *t* test with Welch correction or nonparametric Brown–Forsythe and Welch analysis of variance using the Dunnett T3 multiple comparisons tests were performed using Prism 8 (GraphPad, San Diego, CA) software to analyze the statistical differences between experimental cohorts. Significance was established for *P* values less than .05. All data are presented as means  $\pm$  standard error of the mean (SEM).

### References

- Rahib L, Smith BD, Aizenberg R, Rosenzweig AB, Fleshman JM, Matrisian LM. Projecting cancer incidence and deaths to 2030: the unexpected burden of thyroid, liver, and pancreas cancers in the United States. *Cancer Res* 2014;74:2913–2921.
- Rawla P, Sunkara T, Gaduputi V. Epidemiology of pancreatic cancer: global trends, etiology and risk factors. *World J Oncol* 2019;10:10.
- Erkan M, Michalski CW, Rieder S, Reiser–Erkan C, Abiatari I, Kolb A, Giese NA, Esposito I, Friess H, Kleeff J. The activated stroma index is a novel and independent prognostic marker in pancreatic ductal adenocarcinoma. *Clin Gastroenterol Hepatol* 2008;6:1155–1161.
- Zhang Y, Crawford HC, Pasca di Magliano M. Epithelial-stromal interactions in pancreatic cancer. *Annu Rev Physiol* 2018;81:1–23.
- von Ahrens D, Bhagat TD, Nagrath D, Maitra A, Verma A. The role of stromal cancer-associated fibroblasts in pancreatic cancer. *J Hematol Oncol* 2017;10:76.
- LeBleu VS, Kalluri R. A peek into cancer-associated fibroblasts: origins, functions and translational impact. *DMM Dis Model Mech* 2018;11:1–9.
- Olive KP, Jacobetz MA, Davidson CJ, Gopinathan A, McIntyre D, Honess D, Madhu B, Goldgraben MA, Caldwell ME, Allard D, Frese KK, Denicola G, Feig C, Combs C, Winter SP, Ireland-Zecchini H, Reichelt S, Howat WJ, Chang A, Dhara M, Wang L, Rückert F, Grützmann R, Pilarsky C, Izeradjene K, Hingorani SR, Huang P, Davies SE, Plunkett W, Egorin M, Hruban RH, Whitebread N, McGovern K, Adams J, Jacobuzio-Donahue C, Griffiths J, Tuveson DA. Inhibition of Hedgehog signaling enhances delivery of chemotherapy in a mouse model of pancreatic cancer. *Science* 2009;324:1457–1461.
- Provenzano PP, Cuevas C, Chang AE, Goel VK, Von Hoff DD, Hingorani SR. Enzymatic targeting of the stroma ablates physical barriers to treatment of pancreatic ductal adenocarcinoma. *Cancer Cell* 2012;21:418–429.
- Hwang RF, Moore T, Arumugam T, Ramachandran V, Amos KD, Rivera A, Ji B, Evans DB, Logsdon CD. Cancer-associated stromal fibroblasts promote pancreatic tumor progression. *Cancer Res* 2008;68:918–926.
- Zhang Y, Yan W, Collins MA, Bednar F, Rakshit S, Zetter BR, Stanger BZ, Chung I, Rhim AD, Di Magliano MP. Interleukin-6 is required for pancreatic cancer progression by promoting MAPK signaling activation and oxidative stress resistance. *Cancer Res* 2013;73:6359–6374.
- Matsuo Y, Ochi N, Sawai H, Yasuda A, Takahashi H, Funahashi H, Takeyama H, Tong Z, Guha S. CXCL12/IL-8 and CXCL12/SDF-1 $\alpha$  co-operatively promote invasiveness and angiogenesis in pancreatic cancer. *Int J Cancer* 2009;124:853–861.
- Feig C, Jones JO, Kraman M, Wells RJB, Deonarine A, Chan DS, Connell CM, Roberts EW, Zhao Q, Caballero OL, Teichmann SA, Janowitz T. Targeting CXCL12 from FAP-expressing carcinoma-associated fibroblasts synergizes with anti-PD-L1 immunotherapy in pancreatic cancer. *Proc Natl Acad Sci U S A* 2013;110:20212–20217.
- Özdemir BC, Pentcheva-Hoang T, Carstens JL, Zheng X, Wu CC, Simpson TR, Laklai H, Sugimoto H, Kahlert C, Novitskiy SV, DeJesus-Acosta A, Sharma P, Heidari P, Mahmood U, Chin L, Moses HL, Weaver VM, Maitra A, Allison JP, LeBleu VS, Kalluri R. Depletion of carcinoma-associated fibroblasts and fibrosis induces immunosuppression and accelerates pancreas cancer with reduced survival. *Cancer Cell* 2014;25:719–734.
- Öhlund D, Handly-Santana A, Biffi G, Elyada E, Almeida AS, Ponz-Sarvise M, Corbo V, Oni TE, Hearn SA, Lee EJ, Chio IIC, Hwang C-I, Tiriach H, Baker LA, Engle DD, Feig C, Kultti A, Egeblad M, Fearon DT, Crawford JM, Clevers H, Park Y, Tuveson DA. Distinct populations of inflammatory fibroblasts and myofibroblasts in pancreatic cancer. *J Exp Med* 2017;214:579–596.
- Biffi G, Oni TE, Spielman B, Hao Y, Elyada E, Park Y, Preall J, Tuveson DA. IL1-induced JAK/STAT signaling is antagonized by TGF $\beta$  to shape CAF heterogeneity in pancreatic ductal adenocarcinoma. *Cancer Discov* 2018;9:282–301.
- Mathew E, Brannon AL, Del Vecchio A, Garcia PE, Penny MK, Kane KT, Vinta A, Buckanovich RJ, di Magliano MP. Mesenchymal stem cells promote pancreatic tumor growth by inducing alternative polarization of macrophages. *Neoplasia* 2016;18:142–151.
- Waghray M, Yalamanchili M, Dziubinski M, Zeinali M, Erkkinen M, Yang H, Schradle KA, Urs S, Di Magliano MP, Welling TH. GM-CSF mediates mesenchymal–epithelial cross-talk in pancreatic cancer. *Cancer Discov* 2016;6:886–899.



18. Helms E, Onate MK, Sherman MH. Fibroblast heterogeneity in the pancreatic tumor microenvironment. *Cancer Discov* 2020;10:648–656.
19. Sahai E, Astsaturov I, Cukierman E, DeNardo DG, Egeblad M, Evans RM, Fearon D, Greten FR, Hingorani SR, Hunter T. A framework for advancing our understanding of cancer-associated fibroblasts. *Nat Rev Cancer* Published online 2020;20:174–186.
20. Elyada E, Bolisetty M, Laise P, Flynn WFF, Courtois ETT, Burkhart RAA, Teinor JAA, Belleau P, Biffi G, Lucito MSS, Sivajothi S, Armstrong TDD, Engle DDD, Yu KHH, Hao Y, Wolfgang CLL, Park Y, Preall J, Jaffee EMM, Califano A, Robson P, Tuveson DA. Cross-species single-cell analysis of pancreatic ductal adenocarcinoma reveals antigen-presenting cancer-associated fibroblasts. *Cancer Discov* 2019;9:1102–1123.
21. Sadanandam A, Wilson J, Hammel P, Erkan M, Tosolini M, Kocher HM, Paradis V, Delvecchio FR, Kleeff J, Tijeras-Raballand A, Patil Y, Ragulan C, Cros J, Bousquet C, Neuzillet C, Wilson AS, Apte M, Martinet M. Inter- and intra-tumoral heterogeneity in cancer-associated fibroblasts of human pancreatic ductal adenocarcinoma. *J Pathol* 2019;248:51–65.
22. Hosein AN, Huang H, Wang Z, Parmar K, Du W, Huang J, Maitra A, Olson E, Verma U, Brekken RA. Cellular heterogeneity during mouse pancreatic ductal adenocarcinoma progression at single-cell resolution. *JCI Insight* 2019;4:129212.
23. Dominguez CX, Muller S, Keerthivasan S, Koeppen H, Hung J, Gierke S, Breart B, Foreman O, Bainbridge TW, Castiglioni A, Senbabaoglu Y, Madrusan Z, Liang Y, Junttila MR, Klijn C, Bourgon R, Turley SJ. Single-cell RNA sequencing reveals stromal evolution into LRRRC15+ myofibroblasts as a determinant of patient response to cancer immunotherapy. *Cancer Discov* 2020;10:232–253.
24. Peng J, Sun B-F, Chen C-Y, Zhou J-Y, Chen Y-S, Chen H, Liu L, Huang D, Jiang J, Cui G-S, Yang Y, Wang W, Guo D, Dai M, Guo J, Zhang T, Liao Q, Liu Y, Zhao Y-L, Han D-L, Zhao Y, Yang Y-G, Wu W. Single-cell RNA-seq highlights intra-tumoral heterogeneity and malignant progression in pancreatic ductal adenocarcinoma. *Cell Res* 2019;29:725–738.
25. Bernard V, Semaan A, Huang J, San Lucas FA, Mulu FC, Stephens BM, Guerrero PA, Huang Y, Zhao J, Kamyabi N. Single-cell transcriptomics of pancreatic cancer precursors demonstrates epithelial and micro-environmental heterogeneity as an early event in neoplastic progression. *Clin Cancer Res* 2019;25:2194–2205.
26. Byrnes LE, Wong DM, Subramaniam M, Meyer NP, Gilchrist CL, Knox SM, Tward AD, Ye CJ, Sneddon JB. Lineage dynamics of murine pancreatic development at single-cell resolution. *Nat Commun* 2018;9:1–17.
27. Mathew E, Collins MA, Fernandez-Barrena MG, Holtz AM, Yan W, Hogan JO, Tata Z, Allen BL, Fernandez-Zapico ME, di Magliano MP. The transcription factor GLI1 modulates the inflammatory response during pancreatic tissue remodeling. *J Biol Chem* 2014;289:27727–27743.
28. Rajurkar M, De Jesus-Monge WE, Driscoll DR, Appleman VA, Huang H, Cotton JL, Klimstra DS, Zhu LJ, Simin K, Xu L, McMahon AP, Lewis BC, Mao J. The activity of Gli transcription factors is essential for Kras-induced pancreatic tumorigenesis. *Proc Natl Acad Sci U S A* 2012;109:E1038–E1047.
29. Lau J, Kawahira H, Hebrok M. Hedgehog signaling in pancreas development and disease. *Cell Mol Life Sci* 2006;63:642–652.
30. Mathew E, Zhang Y, Holtz AM, Kane KT, Song JY, Allen BL, di Magliano MP. Dosage-dependent regulation of pancreatic cancer growth and angiogenesis by hedgehog signaling. *Cell Rep* 2014;9:484–494.
31. Schneider RK, Mullally A, Dugourd A, Peisker F, Hoogenboezem R, Van Strien PMH, Bindels EM, Heckl D, Büsche G, Fleck D, Müller-Newen G, Wongboonsin J, Ventura Ferreira M, Puelles VG, Saez-Rodriguez J, Ebert BL, Humphreys BD, Kramann R. Gli1+ mesenchymal stromal cells are a key driver of bone marrow fibrosis and an important cellular therapeutic target. *Cell Stem Cell* 2017;20:785–800.e8.
32. Kramann R, Schneider RK, DiRocco DP, Machado F, Fleig S, Bondzie PA, Henderson JM, Ebert BL, Humphreys BD. Perivascular Gli1+ progenitors are key contributors to injury-induced organ fibrosis. *Cell Stem Cell* 2015;16:51–66.
33. Kramann R, Goettsch C, Wongboonsin J, Iwata H, Schneider RK, Kuppe C, Kaesler N, Chang-Panesso M, Machado FG, Gratwohl S, Madhurima K, Hutcheson JD, Jain S, Aikawa E, Humphreys BD. Adventitial MSC-like cells are progenitors of vascular smooth muscle cells and drive vascular calcification in chronic kidney disease. *Cell Stem Cell* 2016;19:628–642.
34. Zhao H, Feng J, Seidel K, Shi S, Klein O, Sharpe P, Chai Y. Secretion of shh by a neurovascular bundle niche supports mesenchymal stem cell homeostasis in the adult mouse incisor. *Cell Stem Cell* 2014;14:160–173.
35. Kan C, Chen L, Hu Y, Ding N, Li Y, McGuire TL, Lu H, Kessler JA, Kan L. Gli1-labeled adult mesenchymal stem/progenitor cells and hedgehog signaling contribute to endochondral heterotopic ossification. *Bone* 2018;109:71–79.
36. Larsen BM, Hrycaj SM, Newman M, Li Y, Wellik DM. Mesenchymal Hox6 function is required for mouse pancreatic endocrine cell differentiation. *Development* 2015;142:3859–3868.
37. Apte MV, Wilson JS. Dangerous liaisons: pancreatic stellate cells and pancreatic cancer cells. *J Gastroenterol Hepatol* 2012;27:69–74.
38. Apte MV, Haber PS, Applegate TL, Norton ID, McCaughan GW, Korsten MA, Pirola RC, Wilson JS. Periacinar stellate shaped cells in rat pancreas: identification, isolation, and culture. *Gut* 1998;43:128–133.
39. Ahn S, Joyner AL. Dynamic changes in the response of cells to positive hedgehog signaling during mouse limb patterning. *Cell* 2004;118:505–516.
40. Yauch RL, Gould SE, Scales SJ, Tang T, Tian H, Ahn CP, Marshall D, Fu L, Januario T, Kallop D, Nannini-Pepe M, Kotkowi K, Marsters JC, Rubin LL, de Sauvage FJ.

- A paracrine requirement for hedgehog signalling in cancer. *Nature* 2008;455:406–410.
41. Klimstra DS, Longnecker DS. K-ras mutations in pancreatic ductal proliferative lesions. *Am J Pathol* 1994; 145:1547–1550.
  42. Hruban RH, Iacobuzio-Donahue C, Wilentz RE, Goggins M, Kern SE. Molecular pathology of pancreatic cancer. *Cancer J* 2001;7:251–258.
  43. Wen H-J, Gao S, Wang Y, Ray M, Magnuson MA, Wright CVE, Di Magliano MP, Frankel TL, Crawford HC. Myeloid cell-derived HB-EGF drives tissue recovery after pancreatitis. *Cell Mol Gastroenterol Hepatol* 2019; 8:173–192.
  44. Hingorani SR, Petricoin EF, Maitra A, Rajapakse V, King C, Jacobetz MA, Ross S, Conrads TP, Veenstra TD, Hitt BA, Kawaguchi Y, Johann D, Liotta LA, Crawford HC, Putt ME, Jacks T, Wright CV, Hruban RH, Lowy AM, Tuveson DA. Preinvasive and invasive ductal pancreatic cancer and its early detection in the mouse. *Cancer Cell* 2003;4:437–450.
  45. Carriere C, Young AL, Gunn JR, Longnecker DS, Korc M. Acute pancreatitis accelerates initiation and progression to pancreatic cancer in mice expressing oncogenic Kras in the nestin cell lineage. *PLoS One* 2011;6:e27725.
  46. Guerra C, Schuhmacher AJ, Canamero M, Grippo PJ, Verdaguer L, Perez-Gallego L, Dubus P, Sandgren EP, Barbacid M. Chronic pancreatitis is essential for induction of pancreatic ductal adenocarcinoma by K-Ras oncogenes in adult mice. *Cancer Cell* 2007;11:291–302.
  47. Morris JP th, Cano DA, Sekine S, Wang SC, Hebrok M. Beta-catenin blocks Kras-dependent reprogramming of acini into pancreatic cancer precursor lesions in mice. *J Clin Invest* 2010;120:508–520.
  48. Hingorani SR, Wang L, Multani AS, et al. Trp53R172H and KrasG12D cooperates to promote chromosomal instability and widely metastatic pancreatic ductal adenocarcinoma in mice. *Cancer Cell* 2005;7:469–483.
  49. Adams CR, Htwe HH, Marsh T, Wang AL, Montoya ML, Subbaraj L, Tward AD, Bardeesy N, Perera RM. Transcriptional control of subtype switching ensures adaptation and growth of pancreatic cancer. *Elife* 2019; 8:1–25.
  50. Stanger BZ, Hebrok M. Control of cell identity in pancreas development and regeneration. *Gastroenterology* 2013;144:1170–1179.
  51. Chu GC, Kimmelman AC, Hezel AF, DePinho RA. Stromal biology of pancreatic cancer. *J Cell Biochem* 2007; 101:887–907.
  52. Armulik A, Genové G, Betsholtz C. Pericytes: developmental, physiological, and pathological perspectives, problems, and promises. *Dev Cell* 2011;21:193–215.
  53. McNulty RJ. Fibroblasts and myofibroblasts: their source, function and role in disease. *Int J Biochem Cell Biol* 2007;39:666–671.
  54. Darby IA, Laverdet B, Bonté F, Desmoulière A. Fibroblasts and myofibroblasts in wound healing. *Clin Cosmet Investig Dermatol* 2014;7:301.
  55. Costa A, Kieffer Y, Scholer-Dahirel A, Pelon F, Bourachot B, Cardon M, Sirven P, Magagna I, Fuhrmann L, Bernard C, Bonneau C, Kondratova M, Kuperstein I, Zinovyev A, Givel AM, Parrini MC, Soumelis V, Vincent-Salomon A, Mechta-Grigoriou F. Fibroblast heterogeneity and immunosuppressive environment in human breast cancer. *Cancer Cell* 2018; 33:463–479.e10..
  56. Bartoschek M, Oskolkov N, Bocci M, Lövrot J, Larsson C, Sommarin M, Madsen CD, Lindgren D, Pekar G, Karlsson G, Ringnér M, Bergh J, Björklund Å, Pietras K. Spatially and functionally distinct subclasses of breast cancer-associated fibroblasts revealed by single cell RNA sequencing. *Nat Commun* 2018;9:5150.
  57. Li H, Courtois ET, Sengupta D, Tan Y, Chen KH, Goh JLL, Kong SL, Chua C, Hon LK, Tan WS, Wong M, Choi PJ, Wee LJK, Hillmer AM, Tan IB, Robson P, Prabhakar S. Reference component analysis of single-cell transcriptomes elucidates cellular heterogeneity in human colorectal tumors. *Nat Genet* 2017;49:708.
  58. Su S, Chen J, Yao H, Liu J, Yu S, Lao L, Wang M, Luo M, Xing Y, Chen F, Huang D, Zhao J, Yang L, Liao D, Su F, Li M, Liu Q, Song E. CD10+GPR77+ cancer-associated fibroblasts promote cancer formation and chemoresistance by sustaining cancer stemness. *Cell* 2018; 172:841–856.e16.
  59. Sherman MH, Yu RT, Engle DD, Ding N, Atkins AR, Tiriach H, Collisson EA, Connor F, Van Dyke T, Kozlov S, Martin P, Tseng TW, Dawson DW, Donahue TR, Masamune A, Shimosegawa T, Apte MV, Wilson JS, Ng B, Lau SL, Gunton JE, Wahl GM, Hunter T, Drebin JA, O'Dwyer PJ, Liddle C, Tuveson DA, Downes M, Evans RM. Vitamin D receptor-mediated stromal reprogramming suppresses pancreatitis and enhances pancreatic cancer therapy. *Cell* 2014;159:80–93.
  60. McCarroll JA, Phillips PA, Santucci N, Pirola RC, Wilson JS, Apte MV. Vitamin A inhibits pancreatic stellate cell activation: implications for treatment of pancreatic fibrosis. *Gut* 2006;55:79–89.
  61. Hui CC, Angers S. Gli proteins in development and disease. *Annu Rev Cell Dev Biol* 2011;27:513–537.
  62. Hebrok M, Kim SK, Melton DA. Notochord repression of endodermal Sonic hedgehog permits pancreas development. *Genes Dev* 1998;12:1705–1713.
  63. Apelqvist Å, Ahlgren U, Edlund H. Sonic hedgehog directs specialised mesoderm differentiation in the intestine and pancreas. *Curr Biol* 1997;7:801–804.
  64. Lau J, Hebrok M. Hedgehog signaling in pancreas epithelium regulates embryonic organ formation and adult beta-cell function. *Diabetes* 2010;59:1211–1221.
  65. Fendrich V, Esni F, Garay MV, Feldmann G, Habbe N, Jensen JN, Dor Y, Stoffers D, Jensen J, Leach SD, Maitra A. Hedgehog signaling is required for effective regeneration of exocrine pancreas. *Gastroenterology* 2008;135:621–631.
  66. Thomas MK, Rastalsky N, Lee JH, Habener JF. Hedgehog signaling regulation of insulin production by pancreatic beta-cells. *Diabetes* 2000; 49:2039–2047.
  67. El Agha E, Kramann R, Schneider RK, Li X, Seeger W, Humphreys BD, Bellusci S. Mesenchymal stem cells in fibrotic disease. *Cell Stem Cell* 2017;21:166–177.

68. Mederacke I, Hsu CC, Troeger JS, Huebener P, Mu X, Dapito DH, Pradere J-P, Schwabe RF. Fate tracing reveals hepatic stellate cells as dominant contributors to liver fibrosis independent of its aetiology. *Nat Commun* 2013;4:2823.
69. Humphreys BD, Lin S-L, Kobayashi A, Hudson TE, Nowlin BT, Bonventre JV, Valerius MT, McMahon AP, Duffield JS. Fate tracing reveals the pericyte and not epithelial origin of myofibroblasts in kidney fibrosis. *Am J Pathol* 2010;176:85–97.
70. Kanisicak O, Khalil H, Ivey MJ, Karch J, Maliken BD, Correll RN, Brody MJ, Lin S-CJ, Aronow BJ, Tallquist MD. Genetic lineage tracing defines myofibroblast origin and function in the injured heart. *Nat Commun* 2016;7:12260.
71. Xie T, Liang J, Liu N, Huan C, Zhang Y, Liu W, Kumar M, Xiao R, D'Armiento J, Metzger D, Chambon P, Papaioannou VE, Stripp BR, Jiang D, Noble PW. Transcription factor TBX4 regulates myofibroblast accumulation and lung fibrosis. *J Clin Invest* 2016;126:3063–3079.
72. El Agha E, Moiseenko A, Kheirollahi V, De Langhe S, Crnkovic S, Kwapiszewska G, Szibor M, Kosanovic D, Schwind F, Schermuly RT, Henneke I, MacKenzie B, Quantius J, Herold S, Ntokou A, Ahlbrecht K, Braun T, Morty RE, Günther A, Seeger W, Bellusci S. Two-way conversion between lipogenic and myogenic fibroblastic phenotypes marks the progression and resolution of lung fibrosis. *Cell Stem Cell* 2017;20:261–273.e3.
73. Göritz C, Dias DO, Tomilin N, Barbacid M, Shupliakov O, Frisén J. A pericyte origin of spinal cord scar tissue. *Science* 2011;333:238–242.
74. Driskell RR, Lichtenberger BM, Hoste E, Kretzschmar K, Simons BD, Charalambous M, Ferron SR, Haurault Y, Pavlovic G, Ferguson-Smith AC. Distinct fibroblast lineages determine dermal architecture in skin development and repair. *Nature* 2013;504:277.
75. Garcia ADR, Petrova R, Eng L, Joyner AL. Sonic Hedgehog regulates discrete populations of astrocytes in the adult mouse forebrain. *J Neurosci* 2010;30:13597–13608.
76. Nguyen M, Zhu J, Nakamura E, Bao X, Mackem S. Tamoxifen-dependent, inducible Hoxb6CreERT recombinase function in lateral plate and limb mesoderm, CNS isthmus organizer, posterior trunk neural crest, hindgut, and tailbud. *Dev Dyn* 2009;238:467–474.
77. Collins MA, Brisset JC, Zhang Y, Bednar F, Pierre J, Heist KA, Galban CJ, Galban S, di Magliano MP. Metastatic pancreatic cancer is dependent on oncogenic Kras in mice. *PLoS One* 2012;7:e49707.
78. Collins MA, Bednar F, Zhang Y, Brisset JC, Galban S, Galban CJ, Rakshit S, Flannagan KS, Adsay NV, Pasca di Magliano M. Oncogenic Kras is required for both the initiation and maintenance of pancreatic cancer in mice. *J Clin Invest* 2012;122:639–653.
79. Zhang Y, Yan W, Mathew E, et al. CD4+ T lymphocyte ablation prevents pancreatic carcinogenesis in mice. *Cancer Immunol Res* 2014;2:423–435.

---

Received November 20, 2019. Accepted May 14, 2020.

#### Correspondence

Address correspondence to: Marina Pasca di Magliano, PhD, Department of Surgery, University of Michigan, 1500 East Medical Center Drive, 4304 Cancer Center, SPC 5936, Ann Arbor, Michigan 48109. e-mail: marinapa@umich.edu; fax: (734) 615-7424.

#### CRedit Authorship Contributions

Paloma E Garcia (Data curation: Lead; Formal analysis: Lead; Funding acquisition: Supporting; Investigation: Lead; Methodology: Equal; Project administration: Equal; Visualization: Lead; Writing – original draft: Lead; Writing – review & editing: Equal); Maeva Adoumie (Investigation: Supporting; Methodology: Supporting; Writing – review & editing: Supporting); Esther C Kim (Investigation: Supporting; Methodology: Supporting); Yaqing Zhang, MD, PhD (Investigation: Supporting); Michael K Scales (Investigation: Supporting; Visualization: Supporting); Yara S El-Tawil (Investigation: Supporting); Amara Z Shaikh (Investigation: Supporting); Hui-Ju Wen, PhD (Resources: Equal); Filip Bednar, MD, PhD (Conceptualization: Supporting; Funding acquisition: Supporting); Ben L Allen, PhD (Conceptualization: Supporting; Funding acquisition: Supporting; Resources: Supporting); Deneen M Wellik, PhD (Conceptualization: Supporting; Resources: Equal); Howard C Crawford, PhD (Conceptualization: Supporting; Funding acquisition: Supporting; Methodology: Supporting; Resources: Equal; Writing – review & editing: Supporting); Marina Pasca di Magliano (Conceptualization: Lead; Funding acquisition: Lead; Methodology: Lead; Project administration: Lead; Resources: Lead; Visualization: Supporting; Writing – original draft: Supporting; Writing – review & editing: Lead).

#### Conflicts of interest

The authors disclose no conflicts.

#### Funding

This project was supported by the American Cancer Society and the National Cancer Institute of the National Institutes of Health under award numbers R01CA151588, R01CA198074 (M.P.M.), R50CA232985 (Y.Z.), and P30CA046592 by the use of the following Rogel Cancer Center Shared Resources: Flow Cytometry, Cell and Tissue Imaging, and Tissue and Molecular Pathology. This work also was supported by the Cancer Moonshot Initiative U01CA-224145 and an Administrative Supplement to the Rogel Cancer Center Core Grant P30CA046592-28-S2 (M.P.M. and H.C.C.); and by F31-CA221066 and a Rackham Merit Fellowship (P.E.G.). Funded by the Association of Academic Surgery Joel Roslyn Award (F.B.).